National Library of Canada
Bibliothèque nationale du Canada

Canadian Theses Service
Service des thèses canadiennes

Ottawa, Canada
K1A 0N4

NOTICE

The quality of this microform is heavily dependent upon the quality of the original thesis submitted for microfilming. Every effort has been made to ensure the highest quality of reproduction possible.

If pages are missing, contact the university which granted the degree.

Some pages may have indistinct print especially if the original pages were typed with a poor typewriter ribbon or if the university sent us an inferior photocopy.

Previously copyrighted materials (journal articles, published tests, etc.) are not filmed.

Reproduction in full or in part of this microform is governed by the Canadian Copyright Act, R.S.C. 1970, c. C-30.

AVIS

La qualité de cette microforme dépend grandement de la qualité de la thèse soumise au microfilmage. Nous avons tout fait pour assurer une qualité supérieure de reproduction.

S'il manque des pages, veuillez communiquer avec l'université qui a conféré le grade.

La qualité d'impression de certaines pages peut laisser à désirer, surtout si les pages originales ont été dactylographiées à l'aide d'un ruban usé ou si l'université nous a fait parvenir une photocopie de qualité inférieure.

Les documents qui font déjà l'objet d'un droit d'auteur (articles de revue, tests publiés, etc.) ne sont pas microfilmés.

La reproduction, même partielle, de cette microforme est soumise à la Loi canadienne sur le droit d'auteur, SRC 1970, c. C-30.

NL-339 (r. 88/04)

Canada

THE UNIVERSITY OF ALBERTA

Electrokinetic Studies of The Oil/Water and Latex/Water Interfaces

BY

(C) ROSS S. CHOW

A THESIS

SUBMITTED TO THE FACULTY OF GRADUATE STUDIES AND RESEARCH

IN PARTIAL FULFILLMENT OF THE REQUIREMENTS FOR THE DEGREE

OF MASTER OF SCIENCE

DEPARTMENT OF CHEMISTRY

EDMONTON, ALBERTA

FALL 1987

Permission has been granted to the National Library of Canada to microfilm this thesis and to lend or sell copies of the film.

The author (copyright owner) has reserved other publication rights, and neither the thesis nor extensive extracts from it may be printed or otherwise reproduced without his/her written permission.

L'autorisation a été accordée à la Bibliothèque nationale du Canada de microfilmer cette thèse et de prêter ou de vendre des exemplaires du film.

L'auteur (titulaire du droit d'auteur) se réserve les autres droits de publication; ni la thèse ni de longs extraits de celle-ci ne doivent être imprimés ou autrement reproduits sans son autorisation écrite.

ISBN 0-315-40899-5

THE UNIVERSITY OF ALBERTA

RELEASE FORM

NAME OF AUTHOR: Ross S. Chow

TITLE OF THESIS: Electrokinetic Studies on the Oil/Water and Latex/Water Interfaces

DEGREE: Master of Science

YEAR THIS DEGREE GRANTED: 1987

Permission is hereby granted to THE UNIVERSITY OF ALBERTA LIBRARY to reproduce single copies of this thesis and to lend or sell such copies for private, scholarly or scientific research purposes only.

The author reserves other publication rights, and neither the thesis nor extensive extracts from it may be printed or otherwise reproduced without the author's written permission.

Ross Chow

(student's signature)

#304 10745 84 Avenue, Edmonton

(student's permanent address)

Date: 8, July, 1987

THE UNIVERSITY OF ALBERTA

FACULTY OF GRADUATE STUDIES AND RESEARCH

The undersigned certify that they have read, and recommend to the Faculty of Graduate Studies and Research for acceptance, a thesis entitled **Electrokinetic Studies of the Oil/Water and Latex/Water Interfaces** in partial fulfillment of the requirements for the degree of Master of Science.

Thomas L. Hopkins

(Supervisor)

H. W. Brandy

J. J. Cantwell

Date: 29 June, 1957

ABSTRACT

A laser Doppler apparatus, equipped with narrowly gapped platinized platinum electrodes, was used to study the electric properties of two oil-in-water emulsions and a carboxylated latex over a wide range of NaCl concentrations and pH. The oils used were Athabasca bitumen and Moutray conventional crude. It was found that a dilute buffer solution had to be used to control pH drift from occurring on the electrode surface. Analysis of the measured mobility using the Ionizable Surface-Group model [Colloids and Surfaces 15, 35 (1985)] revealed that the negative charge of the oil emulsions was due to the dissociation of carboxylic acids, though Moutray crude oil had only a quarter of acid groups that existed on the bitumen surfaces. Experiments were also conducted in the presence of Ca^{++} and Mg^{++}. The measured mobilities for the oil emulsions were again adequately explained by the model when the ion-binding of the cations with the acid groups was included.

The zeta potentials of the bitumen-in-water emulsions, as calculated from the mobilities were very large (-100 mV in 10^{-2} M NaCl) especially when compared with values for the carboxylated latex (-50 mV in 10^{-2} M NaCl), which had similar surface charge density. This difference was attributed to the surface roughness of the latex particle, which results in a larger value for the location of the shear plane, resulting in a smaller value for the zeta potential. To test this hypothesis the surface roughness of the latex was decreased by heating it above the glass transition temperature. The heat treatment

resulted in a significant increase of the zeta potential. This observation suggests that surface roughness is one of the most important factors in determining zeta potentials from electrophoresis.

In addition, results of measured mobilities of the heat treated latex in NaCl, $CaCl_2$ and $La(NO_3)_3$ solutions below 10^{-4} M and bitumen in 10^{-4} M NaCl and $CaCl_2$ suggest that the computer solution of O'Brien and White over-estimates the electrophoretic relaxation effect at $\kappa a < 100$, where κ is the reciprocal Debye-Hückel length and a is the particle radius.

ACKNOWLEDGEMENTS

I would like to express my sincere thanks to Koichi Takamura. Without his knowledge and patience this work could not have been completed.

I appreciate the help and guidance that I received from my supervisor, Loren Hepler.

I would like to express my gratitude to Dr. H. Kawaguchi for the carboxylated latex sample and Dr. N. Morrow for the Moutray crude oil sample.

I appreciate the financial assistance from the Alberta Research Council.

Many days in the laboratory were made easier by the people with whom I shared the laboratory with, C. McCarthy and D. Maunder.

Finally, I cannnot forget the contribution of my wife Kathy, whose continuous support through this entire project cannot be overestimated.

TABLE OF CONTENTS

Chapter		Page
I	INTRODUCTION	
	Introductory Remarks	2
	The History and Development of the Laser Doppler Apparatus	4
	The Relationship Between Mobility and Zeta Potential	8
	Ionizable Surface-Group Model	12
	Research Conducted for this Thesis	13
	Figures	15
	References	17
II	ELECTROPHORETIC MOBILITIES OF BITUMEN AND CONVENTIONAL CRUDE-IN-WATER EMULSIONS USING THE LASER DOPPLER APPARATUS IN THE PRESENCE OF MULTIVALENT CATIONS	
	Introduction	20
	Experiments	22
	Results	21
	Discussion	37
	Tables	41
	Figures	44
	References	59

III EFFECT OF INNER DOUBLE LAYER STRUCTURE ON THE ELECTROKINETIC POTENTIAL OF LATEX PARTICLES

Introduction 62

Experiments 64

Results 66

Discussion 71

Tables 75

Figures 79

References 84

IV GENERAL CONCLUSIONS AND SUGGESTIONS FOR FURTHER RESEARCH

General conclusions 87

Suggestions for further research 88

APPENDIX I The Laser Doppler Apparatus 89

LIST OF TABLES

Table Number	Heading	Page
II-1	Physical and Chemical Properties of the Oils Used	41
II-2	Composition of the Buffer Solutions Used for Laser Doppler Electrophoresis	42
II-3	Comparison of Electrophoretic Mobilities of Bitumen-in-Water Emulsions Measured by Particle Microelectrophoresis and Laser Doppler Electrophoresis	43
III-1	List of Shear Plane Locations Which Result in Best Fit to Experimentally Observed U^* vs pH Relationships.	75
III-2	Measured Mobilities of the Heat Treated Latex at a Bulk pH of 5.5	76
III-3	Measured Mobilities of Bitumen and Heat Treated Latex in 10^{-4} M Na^+	77
III-4	Measured Mobilities of Bitumen and Heat Treated Latex in 10^{-4} M NaCl in the Presence of 3.0×10^{-5} M $CaCl_2$	78

LIST OF FIGURES

Figure Number	Heading	Page
I-1	The Electrophoretic Relaxation Effect	15
I-2	Zeta Potential and Electrophoretic Mobility Relationships	16
II-1	Measured Particle Size Distributions	44
II-2	Schematic Diagram Showing the Optical Heterodyning and Temperature Control Systems of the Laser Doppler Apparatus	45
II-3	Field Strength of the Electric Field Applied Between the Narrowly Gapped Electrodes	46
II-4	Doppler Spectra for Bitumen Emulsions in the Absence and Presence of Buffer Solutions	47
II-5	Measured Mobility Profile of Bitumen Particles Across the Cell Walls	48
II-6	Comparison of Measured Mobilities of the Bitumen Emulsion Using a Particle Electrophoresis and a Laser Doppler Apparatus	49
II-7	Measured and Calculated Mobilities for the Bitumen Emulsion as a Function of pH in 10^{-3}, 10^{-2}, and 10^{-1} M NaCl	50
II-8	Same as Figure II-7 but in 10^{-4} M NaCl	51
II-9	Same as Figure II-7 but for the Moutray Crude Emulsion	52
II-10	Measured and Calculated Mobilities of Bitumen Emulsion in the Absence and Presence of 10^{-2} M NaCl as a Function of Ca^{++} Concentration at pH 5.5	53
II-11	Same as Figure II-10 but at pH 4, pH 7 and pH 10	54

II-12	Measured and Calculated Mobilities of the Bitumen Emulsion as a Function of pH in 10^{-3} M Ca^{++} and Mg^{++} concentrations in the presence of 10^{-3} M and 10^{-2} M Na^{+}	55
II-13	Measured and Calculated Mobilities of the Moutray Crude Emulsion as a Function of pH in 10^{-3} M Ca^{++} and as a Function of Ca^{++} Concentration.	56
II-14	Measured Mobilities of the Heat Treated Carboxylated Latex Particles With and Without Buffer Solutions as a Function of Ca^{++} Concentration.	57
II-15	Theoretical $U^{*}(\zeta,\kappa a)$ Relationship for the Bitumen Emulsion in the Presence and Absence of 10^{-2} M Na^{+}.	58
III-1	Doppler Spectrum For a Carboxylated Polystyrene-Acrylamide Latex in 10^{-2} M NaCl at pH 10 and a Spectrum for a Mixture of the Original and Heat Treated Latexes at the Same Conditions	79
III-2	Measured and Calculated Electrophoretic Mobilities of the Original and Heat Treated Latexes as a Function of pH	80
III-3	Measured Mobilities of Carboxylated Latex Particles in Aqueous NaCl Solutions Reported by Ottewill and Shaw	81
III-4	Plot of Experimental Results of U^{*} vs κa for the Heat Treated Latex as Shown in Table III-1.	82
III-5	U^{*} vs ζ Relationships for $26<\kappa a<30$ in NaCl Solutions Estimated From the Measured U^{*} of a Bitumen Emulsion and The Heat Treated Latex.	83

CHAPTER I

INTRODUCTION

Introductory Remarks

Today, society has a strong dependence on petroleum products. The present estimates of the reserves of conventional crude in Canada ($1.4-2.0 \times 10^9$ m^3) place the lifetime of the reserve at 7-10 years. In order to become self sufficient, it will be necessary to develop alternate sources of oil. The best possibility is the oil present as bitumen in Alberta's oil sands. These sands are estimated to contain 1.94×10^{11} m^3 of oil. At the present time there are two surface mining megaprojects and several smaller in situ projects exploiting the resource.

The importance that the electric properties of the bitumen/water interface have on bitumen recovery has been clearly shown (1). The double layer force plays an important role in such processes as emulsion stability (2,3), the hot water process (a technique used to separate the bitumen from the surface mined oil sand) (4), and in situ oil production (5). It is important to develop a theoretical model that accurately predicts the electric properties of the bitumen/water interface if maximum efficiency is to be attained in the aforementioned processes. For aqueous NaCl solutions of varying pH this has been accomplished by applying the Ionizable Surface-Group model to the bitumen/water interface (6). In that study, the validity of this theory was tested by comparing the theoretically predicted electrophoretic mobilities with those obtained by the experimental technique of electrophoresis.

Electrophoresis is a technique that is used to characterize colloidal materials. The principle of the technique is quite simple. By measuring the velocity of a particle under the influence of an electric field, information about the electric properties of the particle/solution interface is obtained. In conventional electrophoresis, the movement of the particles is observed through a microscope, with the velocity determined by timing over a grid of known dimension. The quantity that comes directly from the measurements is the electrophoretic mobility, which is the velocity of the particle divided by the strength of the electric field. One problem with conventional electrophoresis is that the operator has no idea of the size of the particle whose mobility is being determined. As discussed in the following section on zeta potential, under conditions of strong electrophoretic relaxation, the mobility of a particle is strongly dependent on its size. Under these conditions it is difficult to compare the theoretically predicted mobilities with the measured mobilities if the particle size distribution of the emulsion is wide. Such is the case with the bitumen-in-water emulsion.

An alternative to conventional electrophoresis is laser Doppler electrophoresis, in which the velocities of the particles are determined from the frequency shifts of the scattered light. The problem is that the small velocities obtained in electrophoresis (e.g. $<100\ \mu ms^{-1}$) produce small frequency shifts (<100 Hz). A shift of this magnitude is not easily distinguished from the incident laser frequency ($\sim 10^{15}$ Hz). Detection of this shift is accomplished by mixing shifted and unshifted light to obtain a beat frequency that is equal to the

frequency shift. By using laser Doppler electrophoresis, it was found that it is possible to correlate the mean particle size of the bitumen-in-water emulsion with the mobility observed (this thesis chapter II).

In this chapter, the history of the development of laser Doppler electrophoresis will be described. This is followed by a discussion of the relationship between the electrophoretic mobility and the zeta potential, a brief description of the Ionizable Surface-Group model, and the research performed in this thesis.

The History and Development of Laser Doppler Electrophoresis

The earliest report of combining laser light scattering with electrophoresis was by Ware and Flygare in 1971 (7). In that study a conventional electrophoresis cell was used in conjunction with laser light scattering to measure the electrophoretic mobility of bovine serum albumin. It was found that reasonable signals could be obtained only if the field applied was an order of magnitude higher than commonly used in conventional microelectrophoresis. One problem with the large electric field was that the passage of the current created a large amount of heat. This was controlled by performing the experiments at 10° C and by pulsing the electric field, switching the polarity for every pulse.

An additional problem that was not addressed in that paper was the electroosmotic effect. Since the cell wall/solution is charged, the concentration of counterions in the vicinity of the surface is higher than in the bulk. When subjected to an electric field the counterions

will migrate toward the oppositely charged electrode, carrying some of the water associated with them. Since the cell is a closed system, the flow of solution along the walls creates a counterflow through the middle of the cell. These fluid velocities, coupled with the electrophoretic mobility of the particles creates an apparent flow profile that is parabolic. To eliminate this, measurements of electrophoretic mobility are conducted on a plane where the opposing fluid velocities cancel, the so-called stationary plane.

More recently, Haas and Ware (8) reported a new cell design that involved the use of hemicylindrical silver-silver chloride electrodes that were separated by a small (~3 mm) spacer. This cell had the advantages of small sample volume and improved heat dissipation. With this cell, electroosmosis was minimized by coating the walls with a protein. The idea was that the low charge of the protein would minimize the electroosmotic effect. The measured flow profile was indeed very uniform as compared to that observed without the protein coating. The stability of this coating is questionable and this procedure is not recommended for general use (9).

An alternate way of generating high fields is to use a pair of inert, narrowly gapped electrodes. This idea was conceived by Uzgiris who first reported this configuration in 1972 (10). The narrowly gapped electrodes have the following advantages: high fields are easy to attain, heat dissipation is improved because of the high thermal conductivity of the metal, and there are no signs of electroosmosis (11,12). One problem with narrowly gapped electrodes is that the electrode surfaces are very close to all of the sample and any surface

reaction on the electrode may alter the electrophoretic mobility of the sample (13, this thesis chapter II).

In 1980, Uzgiris and Cluxton (14) reported a simple configuration that could be used to attain scattering at angles greater than 15°. Before this, most electrophoretic light scattering was done at angles less than 10°. The reason for the development of the larger scattering angle is reviewed in that article and will be briefly explained. The majority of experimenters considered Brownian motion to be the main reason for the broadening of Doppler peaks. The full width at half height would be given by (14):

$$\Delta f = \frac{DK^2}{\pi} \qquad [1]$$

where D is the diffusion constant that is given by $kT/(6\pi\eta a)$ for a sphere of radius a immersed in a medium of viscosity η, k is the Boltzmann constant and T is the absolute temperature. K is the scattering vector that is given by $(4\pi n/\lambda)\sin(\theta/2)$ for radiation of wavelength λ scattered at angle θ in a medium of refractive index n.

The Doppler shift expected from a particle with electrophoretic mobility U under the influence of electric field E is given by (14):

$$\delta f = \frac{UEK}{2\pi} \qquad [2]$$

A resolution factor is defined as the ratio of frequency shift to the width at half height:

$$\frac{\delta f}{\Delta f} = \frac{UE}{2DK} = \frac{3}{4\pi} \frac{\lambda \eta a UE}{nkT} \frac{1}{\sin(\theta/2)} \qquad [3]$$

This equation implies that the Doppler peaks will become infinitely thin as the scattering angle approaches zero.

Uzgiris (14) suggested that Brownian motion was not the sole source of peak broadening and problems such as spectrum analyzer resolution, effects due to switching the field, field inhomogeneities and convective motion also contributed to peak width. His estimate of these effects would increase the peak width by approximately 1.0 Hz, an amount that becomes significant as the scattering angle decreases. This residual broadening was added to the denominator of the resolution factor. Assuming a reasonable electrophoretic velocity for red blood cells (UE = 20 μms^{-1}), he plotted the resolution factor against the scattering angle. The resulting curve showed the maximum resolution at $\theta = 40°$; this angle would be the ideal angle for that particle size ($a \sim 5\ \mu m$). He extended this plot in a following article (12), and plotted the ideal scattering angle as a function of particle size for two values (0.5 and 1.0 Hz) of residual broadening. If some idea of the particle size is available, the experimenter can pick the ideal angle at which to perform the laser Doppler electrophoresis.

Most of these effects are reported in an excellent review article written by Uzgiris (12).

The Relationship Between Electrophoretic Mobility and Zeta Potential

Although some information can be inferred from electrophoretic mobility (e.g., nature of the surface group) the zeta potential, which can be related to the electrophoretic mobility, is the parameter of most interest. The zeta potential is not the surface potential of the particle but the potential a certain distance away from the surface. The plane corresponding to this distance is called the surface of shear or shear plane. The reason that the surface potential cannot be measured directly by electrophoresis is that there is a small amount of suspending medium immovably associated with the surface. As the particle moves under the influence of the electric field it is the potential at the shear plane that influences the electrophoretic mobility. Obviously, the distance to the shear plane has great bearing on the value of the zeta potential. It has been suggested (this thesis chapter II) that for smooth surfaces this distance is of the order of 0.6 nm.

In order to obtain the electrophoretic mobility and zeta potential relationship, the electrophoretic relaxation effect must be taken into account. When a particle and its surrounding double layer are subjected to an electric field the cloud distorts to the shape shown in Figure I-1. This distorted cloud creates its own electric field that opposes the motion of the particle. This is the electrophoretic relaxation effect. The magnitude of the effect is proportional to the thickness of the double layer in relation to the size of the particle.

This can be expressed as the parameter κa where a is the particle radius and κ (also referred to as the Debye-Hückel reciprocal length) is given by:

$$\kappa = [e^2 \Sigma n_i z_i^2 / (\epsilon k T)]^{1/2} \qquad [4]$$

where n_i and z_i are the number of ions per unit volume and valency of ionic species i, respectively, e is the electronic charge, and ϵ is the permittivity of the medium. Thus the observed electrophoretic mobility is not only a function of the zeta potential, but is also dependent on the size of the particle.

Within the limit of small ($\kappa a < 1$) and large ($\kappa a > 300$) κa there exist simple equations that will adequately relate the zeta potential, ζ, and electrophoretic mobility, U. The reason for this is that the particle can be treated as a point charge (small κa) and as an infinitely large flat surface (large κa) in relation to the size of the double layer. The equations are:

$$U = \zeta \epsilon / (1.5\eta) \qquad (\kappa a < 1) \qquad [5]$$

$$U = \zeta \epsilon / \eta \qquad (\kappa a > 300) \qquad [6]$$

Most electrophoretic measurements, however, are conducted in the critical range ($1 < \kappa a < 300$) where the magnitude of the relaxation effect is sufficient that the exact relationship between zeta potential and electrophoretic mobility must be calculated. A variety of researchers have worked on this problem. The solution involves the balancing of

all the forces involved. These are the driving force on the particle (electrical), the electrophoretic relaxation effect (electrical), the hydrodynamic drag due to the particle (hydrodynamic), and the drag due to the ion cloud (hydrodynamic).

Overbeek (15) made the first successful attack on this problem which was followed by an independent investigation by Booth (16). Both researchers obtained relatively similar equations and represented the mobility in terms of the zeta potential multiplied by a function that was dependent on the zeta potential and κa. Wiersema (17) numerically solved the differential equations involved and provided tabulated and graphical information for the conversion of mobility to zeta potential. There were problems, however, in obtaining convergence to the numerical solution with zeta potentials greater than 100 mV. Derjaguin and Dukhin (18) reported an equation and presented it in such a form that it appeared to be the Smoluchowski equation (eqn. [6]) with a correction term for the relaxation effect. They presented results of the calculation with zeta potentials up to 200 mV.

In 1978, O'Brien and White (19) reported a computer solution that calculated the relationship between the mobility and zeta potential for any combination of ions in solution. Their idea was to break the problem into two parts; the force required to hold a particle stationary in flow, and the force required to hold a particle stationary in an applied electric field. The appropriate differential equations were solved for each situation and by superimposing the solutions and the boundary conditions, the solution to the original

problem resulted. On request, O'Brien and White will provide a computer program that solves the appropriate equations. This is the method by which most colloid chemists calculate the relationship between the mobility and the zeta potential. It does, however, require access to a large computer and considerable computation time. O'Brien and Hunter (20) reported a very simple equation that gave accurate values for the mobility and the zeta potential at modest values of κa ($\kappa a > 100$). Its strength is that a hand calculator can be used to do the calculation. Oshima (21) reported an equation somewhat more complex, which could be used to give results to within 1% of the computer solution of O'Brien and White (19) (under the constraint of $\kappa a \geq 10$ and solutions containing symmetrical electrolytes) with the advantage of reduced computing time.

The relationships between mobility and zeta potential for κa = 8.3, 26 and 83 are shown in Figure I-2. For a particle radius of 0.8 μm this corresponds to NaCl concentrations of 10^{-5}, 10^{-4}, and 10^{-3} M. Alternatively, it is possible to express this as a constant NaCl concentration of 10^{-4} M and particle radii of 0.25, 0.80 and 2.5 μm. These were calculated using the computer solution of O'Brien and White, at 30° C. Several things are striking about the curves. For each condition shown, there exists a maximum mobility. The maximum occurs because the driving force is proportional to the zeta potential while the retarding force is proportional to the square of the zeta potential. The existence of the maximum also complicates the conversion of electrophoretic mobility to zeta potential. For an experimentally measured electrophoretic mobility, there exist two

possible values for the zeta potential. The results also show that as κa is decreased, the curve begins to flatten at zeta potentials greater than 100 mV. This means that at low κa for any zeta potential greater than 100 mV the electrophoretic mobility observed will be the same.

Experimentally it is difficult to establish the relationship between the mobility and zeta potential. The problem is that a suitable particle is not readily available. Ideally, the particle should be monodisperse, spherical, and have a zeta potential (up to 200 mV) that can be altered in some systematic fashion without changing κa. For the most part, this means changing particle size. Ottewill and Shaw (22) did this with five different polystyrene latexes of different sizes. With monovalent electrolytes, they obtained maximum mobilities that were similar to the maxima predicted by theory. Using bivalent electrolytes, however, some of the mobilities exceeded the maxima predicted by theory. Recently, a more rigorous test of the theory was accomplished (this thesis chapter III). The results show that the computer solution overestimates the relaxation effect at low κa and high zeta potential.

The Ionizable Surface-Group Model

One method to describe the electric properties of the interface is the Ionizable Surface-Group model (23). Previously, the model was used to predict the electrophoretic mobilities of a bitumen-in-water emulsion (6, this thesis chapter II). When applied to oil, the model assumed that the surface charge arose from the dissociation of carboxyl

groups at the interface. The degree of dissociation (hence, surface charge) was regulated by the pH in the vicinity of the surface, the dissociation constant of the group and the total number of surface groups. An interesting result was that the pH at the surface is lower than the pH in the bulk due to the interaction between the negatively charged surface and the hydrogen ions in solution. To preserve electrical neutrality, this surface charge was equated to the diffuse double layer charge as given by Gouy-Chapman theory. The result is an equation relating between bulk pH and surface potential in terms of the dissociation constant of the group, pKa, the total number of surface groups, Ns, and the ion concentration. In order to calculate the zeta potential, the value for the shear plane is assumed and the potential at that surface is calculated using the Gouy Chapmann expression for the potential as a function of distance from a charged surface. With proper accounting for the relaxation effect, the electrophoretic mobility can be calculated. Thus, the electrophoretic mobility as a function of bulk pH can be calculated theoretically and compared with experimental results.

Research Conducted for this Thesis

In the second chapter, a description of the laser Doppler electrophoresis apparatus used is provided, with attention given to the problem of pH drift that occurred on the surface of the electrodes. This was solved by using a dilute buffer solution. The Ionizable Surface-Group model was used to predict the electrophoretic mobilities of a conventional crude oil and Athabasca bitumen as a function of pH

in solutions with NaCl concentrations varying from 10^{-3} to 10^{-1} M. The results reconfirm previous findings (6) that the surface charge on both types of oil originates from the dissociation of carboxyl groups present as natural surfactants in the oil. Experiments were also done in the presence of calcium ion. To apply the model sucessfully, it was found that an ion-binding constant was needed to account for the interaction between the calcium ion and the surface group.

In the third chapter, the zeta potentials (calculated from the electrophoretic mobilities) of a carboxylated latex were determined and compared to those of bitumen. The latex was chosen as it had similar surface group density and size as the bitumen emulsion referred to in the second chapter. The zeta potentials obtained were much lower than those for bitumen. It was thought that this may be due to a roughness on the surface of the particle which resulted in a larger shear plane value (this results in a smaller zeta potential). To test this hypothesis, the surface roughness was modified by heating the latex above the glass transition temperature of the polymer. The zeta potentials of the heat treated latex were similar to those of bitumen. The heat treated latex was then used to study the electrophoretic relaxation effect.

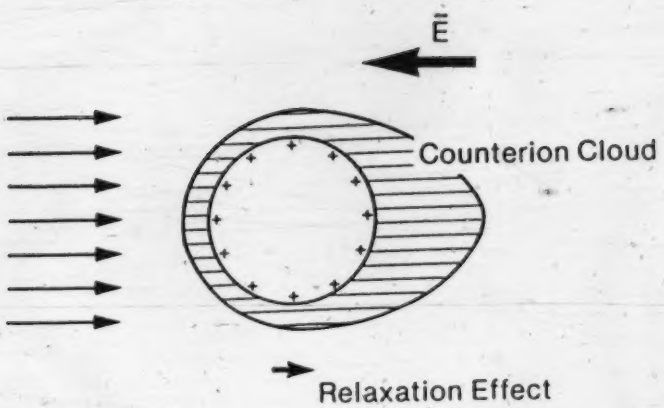

Figure I-1 The electrophoretic relaxation effect. When a particle and its surrounding double layer are exposed to the electric field, E, the counterion cloud distorts to the shape shown. The distorted cloud creates its own electric field that opposes the motion of the particle.

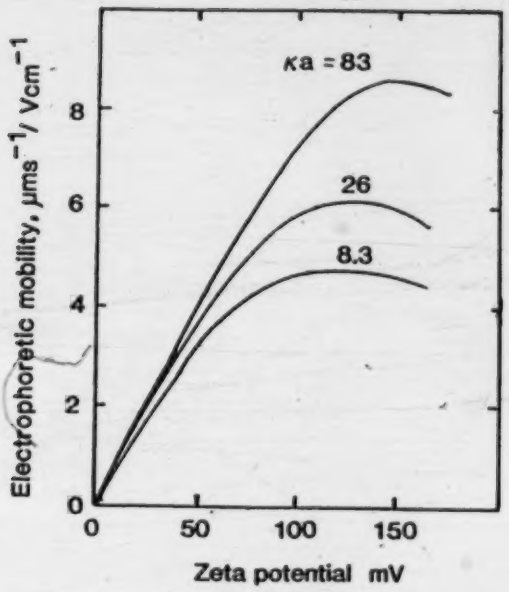

κa	a = 0.8 μm [NaCl], M	[NaCl] = 10^{-4} M a, μm
8.3	10^{-5}	0.25
26	10^{-4}	0.80
83	10^{-3}	2.5

Figure I-2 The theoretical relationship between electrophoretic mobility and zeta potential for κa = 8.3, 26, and 83. The corresponding combinations of electrolyte concentration and particle size are shown in the table. For each κa there is a maximum mobility that can be attained. The existence of this maximum also results in the fact that for an experimentally observed electrophoretic mobility, there exist two possible values of zeta potential.

REFERENCES

1. Takamura, K., AOSTRA Journal of Research 2, 1 (1985).
2. Takamura, K., Energy Processing Canada 74, 29 (1982).
3. Takamura, K., Chow, R.S., and Tse, D.L.; Proc. Sym. on Flocculation in Biotechnology and Separation Systems, San Francisco CA, July 1986.
4. Schram, L.L. and Smith, R.G., Colloids and Surfaces 14, 67 (1985).
5. Takamura, K. and Chow, R.S., J. Can. Petr. Tech. 22, 22 (1983).
6. Takamura, K. and Chow, R.S., Colloids and Surfaces 15, 35 (1985).
7. Ware, B.R. and Flygare, W.H., Chemical Physics Letters 12, 81 (1971).
8. Haas, D.D. and Ware, B.R., Analytical Biochemistry 74, 175 (1976).
9. Hunter, R.J., "Zeta Potential in Colloid Science" Academic Press, New York, 1981.
10. Uzgiris, E.E., Opt. Comm. 6, 55 (1972).
11. Uzgiris, E.E., Rev. Sci. Instrum 45, 74 (1974).
12. Uzgiris, E.E., Adv. Colloid and Interface Sci. 14, 75 (1981).
13. Uzgiris, E.E. and Kaplan, J.H., Rev. Sci. Instrum. 45, 120 (1974).
14. Uzgiris, E.E. and Cluxton, D.H., Rev. Sci. Instrum. 51, 44 (1980).
15. Overbeek, J. Th. G., Adv. Colloid Sci. 3, 97 (1950).
16. Booth, F., Proc. Roy. Soc. London A203, 514 (1950).
17. Wiersema, P.H., Loeb, A.L., and Overbeek J. Th. G., J. Colloid and Interface Sci. 22, 78 (1966).
18. Derjaguin, B.V. and Dukhin, S.S. in "Surface and Colloid Science" (E. Matijevic ed.) Vol. 7, p. 307, John Wiley, New York, 1974.
19. O'Brien, R.W. and White, L.R., J. Chem. Soc. Faraday Trans. 2 74, 1607 (1978).
20. O'Brien, R.W. and Hunter, R.J., Can. J. Chem. 59, 1878 (1981).

21. Oshima, H., Healy, T.W., and White, L.R., J. Chem. Soc. Faraday Trans. 2 79, 1613 (1983).

22. Ottewill, R.H. and Shaw, J.N., J. Electroanal. Chem. 37, 133 (1972).

23. Healy, T.W. and White, L.R., Adv. Colloid and Interface Sci. 9, 303 (1978).

CHAPTER II

ELECTROPHORETIC MOBILITIES OF BITUMEN AND CONVENTIONAL CRUDE-IN-WATER EMULSIONS USING THE LASER DOPPLER APPARATUS IN THE PRESENCE OF MULTIVALENT CATIONS*

*A version of this chapter has been submitted for publication. Chow, R.S. and Takamura, K., Journal of Colloid and Interface Science, 1987.

INTRODUCTION

It was shown in a previous paper (1) that the electric properties of the bitumen/water interface can be predicted using the Ionizable Surface-Group model over a wide range of pH from 4 to 11, and in NaCl concentrations from 10^{-4} to 10^{-1} M. The results indicated that the bitumen surface is negatively charged due to the dissociation of carboxyl groups belonging to surfactants naturally present in bitumen. The study also demonstrated the existence of a maximum in the mobility at high zeta potentials due to the electrophoretic relaxation effect as predicted by O'Brien and White (2). However, an exact comparison between the measured and predicted mobility relationship, $U(\zeta,\kappa a)$ at $\kappa a<60$ (where ζ is the zeta potential, κ^{-1} is the Debye-Hückel length and a is the particle radius), was difficult because of uncertainty in the measured mean particle size for the electrophoresis using the conventional particle microelectrophoresis apparatus. It was found (1) that there was a tendency to neglect small particles when a polydisperse sample was used.

Recently several authors have reported on the use of a laser Doppler apparatus (3-6) for electrophoresis measurements, since the mobilities of a large number of particles can be measured rapidly. In the present paper we used a laser Doppler apparatus to compare the electric properties of bitumen and Moutray conventional crude oil emulsions in aqueous NaCl solution. These two oil samples were chosen to represent crude oils having significantly different values of acid number (amount of organic acids in the crude oil) and asphaltene

content. Experiments were also conducted in solutions containing various concentrations of multivalent cations in the presence and absence of NaCl.

It is known (7-10) that the electric properties of the oil/water interface affect the flow behavior of emulsions, changes in reservoir wettability, and thus oil recovery. Therefore, it is particularly important to develop an appropriate model, which satisfies both accuracy and simplicity, to describe the electric properties at reservoir conditions in the presence of various ion species. Pashley demonstrated, in a series of papers (11-13), that simple mass action equations adequately describe the ion exchanges occurring on clay mineral surfaces, and successfully explain the double layer repulsive forces acting between mica surfaces. Applicability of his equations to the crude oil/water interface will be discussed in detail.

Before describing our experimental results we will discuss the problem of pH drift encountered during laser Doppler electrophoresis equipped with narrowly gapped electrodes.

EXPERIMENTS

1. Crude Oil Samples:

Samples used for this study comprised bitumen extracted with toluene from Athabasca oil sand, and Moutray conventional crude oil. Physical and chemical properties of these samples are listed in Table II-1. The residual toluene content in the bitumen was below 1%.

2. Preparation of Emulsions:

(a) Bitumen-in-Water Emulsion. A 5-g sample of bitumen was dispersed in 100 ml of water at 70°C using a handheld homogenizer (Chase Logman Corp., Hixville, NY). The pH of the water was adjusted to 10 with NaOH. The dispersion was passed through the homogenizer twice, resulting in droplets having a radius between 1 and 10 μm. However, the procedure could disperse only ~25% of the original bitumen in the water. Particles bigger than 6 μm radius were further reduced by letting the dispersion stand for five hours. The final emulsion contained approximately 1% bitumen with a mean particle radius of 0.9 μm.

(b) Moutray Crude-in-Water Emulsion. A 4-ml sample of crude oil was dispersed in 100 ml of water at room temperature using the same procedure as above. Nearly 100% of the crude oil was dispersed in the water, having particle radii ranging between 1 and 8 μm with a mean value of 1.6 μm.

The size distributions for both emulsion samples were determined by Coulter Counter and are shown in Figure II-1.

A 100-μl sample of each emulsion was then diluted in 20 ml of water. The pH of the water was controlled with dilute buffer solutions with compositions as shown in Table II-2. The buffer solutions were used to prevent pH drift from occurring on the electrode surface. The Na^+ concentration of the dispersion was adjusted to a desired value by adding a NaCl solution, as checked using a sodium ion selective electrode with a calomel reference. In some experiments, $CaCl_2$ or $MgCl_2$ solutions were also used to prepare dispersions containing a desired Ca^{++} or Mg^{++} concentration.

3. Laser Doppler Apparatus:

The laser Doppler apparatus used for this study was based on the design described by Uzgiris (4). The configuration of the optical heterodyning and temperature control systems is shown schematically in Figure II-2. The He-Ne laser beam (Spectra Physics Model 124b, Santa Clara, CA) was split into main and reference beams of 99.5% and 0.5% intensity, respectively, by a beam splitter (TSI Inc., Model 9115-2, St. Paul, MN). A focusing lens (TSI 9117) focused these beams between a pair of narrowly gapped (1.8 mm) platinized platinum electrodes placed in a 2 x 10 mm cuvette (ICL Inc., Type 26, Elizabeth, NJ). The cuvette was held in an aluminum block that was thermostatically controlled using a solid state heat pump (Bailey Instruments, Model TS-2ER, Saddle Brook, NJ). It was possible to maintain constant temperatures from 5°C to 60°C with an accuracy of ±0.1°C. A portion of

the main beam scattered by the moving particles was mixed with the reference beam and steered into a photomultiplier tube (Hamamatsu Inc., Model R928, Middlesex, NJ) through pinholes. The signal from the photomultiplier tube was amplified (Tektronix AM502, Beaverton, OR) and processed by a spectrum analyser (Hewlett Packard 3582A, Palo Alto, CA).

An electric field was applied between the electrodes in a square wave form at a frequency of 1 Hz using a frequency generator (Tektronix FG501A). The field strength was continuously monitored by a data acquisition system (Hewlett Packard 3421A). As shown in Figure II-3, approximately 0.2 seconds was required to obtain a constant field strength at high electrolyte concentration (0.1 M NaCl). The spectrum analyser was delayed 0.25 seconds to acquire the signal.

Normally sixty-four wave forms over a 0-50 Hz span were acquired and averaged. The time for the total measurement was approximately five minutes. The Doppler spectra from bitumen particles with and without the buffer solution are shown in Figure II-4. The measured spectrum was curve fitted using the least square spline method, then numerically differentiated, and finally the characteristic frequency shift, Δf, was calculated from the root of this differential equation. The electrophoretic mobility, U, was calculated from Δf using the relation (3,4);

$$U = \frac{(\lambda/2n)\Delta f}{E \sin(\theta/2)} \qquad [1]$$

where λ is the wavelength of the laser beam (632 nm), n is the refractive index of water, E is the electric field strength and θ is the scattering angle of 16.2 degrees for our apparatus. All mobility measurements were conducted at 25°C.

A particle electrophoresis apparatus (Rank Brothers, MK II, Cambridge, England) was also used for comparison.

RESULTS

1. Mobility Profile Across the Electrophoresis Cell Walls:

The main advantage of using narrowly gapped electrodes is the uniform mobility profile across the cell walls normal to the electric field, in comparison to the parabolic profile obtained in conventional widely-spaced electrodes (3,4). The mobility profile of bitumen particles in our cell assembly was measured visually at the midpoint between the electrodes. The cell assembly was placed in a Rank Brothers apparatus and the particle motion was video-recorded through a microscope. The mobility was then measured using frame-by-frame analysis. In this way the particle mobility could be determined under the electric field alternating at a frequency of 1 Hz. As seen in Figure II-5, the measured mobility was flat in the middle 60% of the cell and decreased gradually near both walls.

2. Variation in Bitumen-in-Water Emulsion Samples:

The bitumen-in-water emulsion used in a previous study (1) was produced during the in situ steam injection process, whereas in this study toluene- extracted bitumen was dispersed in water. The different sources of bitumen, especially the presence of trace quantities of solvent in the present bitumen, may affect the electric properties of the bitumen/water interface. Electrophoretic mobilities of the toluene extracted bitumen-in-water emulsion were first measured in 10^{-2} M NaCl

as a function of pH using the Rank Brothers particle electrophoresis apparatus.

Although the bitumen particles were negatively charged, the mobilities reported here are the absolute values of the reduced electrophoretic mobility, U^*, as defined by;

$$U^* = \frac{3\, e\eta|U|}{2\, \epsilon kT} \qquad [2]$$

where e is the electron charge, η and ϵ are the viscosity and permittivity of water, respectively, k is the Boltzmann constant, and T is the absolute temperature.

Measured mobilities are shown in Figure II-6 as open circles and compared with those predicted from the Ionizable Surface-Group model, assuming that the charge of the bitumen/water interface is due to the dissociation of carboxyl groups (1). As seen in Figure II-6, the Ionizable Surface-Group model explains the measured mobility using the same material constants of $N_s = 2 \times 10^{18}\ m^{-2}$, $pK_a = 4.5$ and $x = 0.6$ nm as for the previous study (1). N_s is the total surface density, pK_a is the dissociation constant of functional groups, and x is the location of the shear plane. It is seen that the emulsion used in this study has electric properties similar to the one used in the previous work.

3. pH Drift at the Electrode Surface:

Surprisingly, in spite of the above observation, completely different results (solid circles in Figure II-6) were obtained when the laser Doppler apparatus was used to measure the mobility of the same

emulsion. Mobilities measured by the laser Doppler electrophoresis showed almost no increase in mobility as the pH of the solution changed from 4 to 9. The mobilities determined by the video-recording technique, described in the mobility profile section, agreed with those measured by the laser Doppler apparatus. Therefore this difference in mobility is not due to the velocity determination by the laser Doppler technique.

Close inspection of Figure II-6 indicates that the mobilities determined by the laser Doppler apparatus correspond roughly to the predicted mobility at pH 5.5 (pH of water with dissolved CO_2) even though they were measured at above and below this pH. This observation suggests that the solution might be undergoing pH drift below and above pH 5.5 during the measurement. The decline in pH was confirmed using a phenol red solution. An electric field of ~800 Vm^{-1} was applied in 10^{-2} M NaCl solution at pH 10. The yellow color (pH>8.0) of the original phenol red solution changed to red (pH<6.6) within 100 seconds after the field was applied, presumably due to some surface reaction in the vicinity of the electrodes. The exact mechanism was not investigated further. Uzgiris et al., (14) reported that the problem of the decline in solution pH could be solved by coating the electrodes with bovine serum albumin. Our experiments showed that the coating did not alleviate the problem even though our field strength was much lower than his (800 Vm^{-1} vs 3 kVm^{-1}).

It is known (15) that platinized platinum electrodes have a strong tendency to adsorb various ions. The increase in pH at pH<5.5 may be explained due to hydrogen ion adsorption on the electrode surface. Indeed, when the electrodes were equilibrated in a portion of the solution to be tested for one hour before the measurement, changing the

solution every fifteen minutes, the problem of the pH drift was resolved.

To eliminate the pH drift, it was decided to use a dilute buffer solution of known cation concentration. The buffer solutions used for NaCl concentrations above 10^{-3} M NaCl are listed in Table II-2. Na^+ concentrations of these buffer solutions measured using a Na^+ selective electrode were approximately 5×10^{-4} M. The Na^+ concentration of the emulsion was further altered to the desired value by adding NaCl. In addition, the electrodes were platinized often (every two days) to maintain the optimum working condition. The Doppler spectra of the emulsion in 10^{-2} M NaCl at pH 9.0 in the presence and absence of the buffer solution are shown in Figure II-4. As seen, the spectrum obtained in the buffer solution is significantly sharper than that without the buffer, due to the fact that there is no change in the mobility during the measurement.

The electrophoretic mobilities of the bitumen-in-water emulsion in the buffer solutions of 10^{-3} and 10^{-2} M Na^+ were again measured using the laser Doppler apparatus, and also using the Rank Bros. particle electrophoresis apparatus in the same Na^+ concentrations with and without the buffer solutions. Results listed in Table II-3 show excellent agreement of the mobilities measured by the two instruments, demonstrating that the buffer solutions do not influence the mobility of the bitumen particles at our experimental conditions.

4. Electrophoretic Mobilities in NaCl Solutions:

(a) Bitumen-in-Water Emulsion. Figure II-7 summarizes the mobilities measured for the bitumen-in-water emulsion in Na^+ concentrations of 10^{-3}, 10^{-2} and 10^{-1} M as a function of solution pH. Symbols represent the measured mobilities and the lines are calculated from the Ionizable Surface-Group model as discussed in the previous paper (1). The formula derived by Ohshima et al., (16) for a mean particle radius of 0.9 μm was used for the $U(\zeta,\kappa a)$ relation. The reproducibility of the measurement, which was independent of the electrolyte concentration and pH, was approximately ±0.25 of U^* (indicated by the error bar in the figure). The measured and calculated mobilities are in excellent agreement, thus confirming the applicability of the Ionizable Surface-Group model to describe the electric properties of the bitumen/water interface.

The mobilities were also calculated using a particle size of 1.5 μm, shown by dashed lines in Figure II-7. The mobilities calculated for 10^{-3} M Na^+ are now higher than the measured U^* because of the smaller degree of the electrophoretic relaxation effect at the larger value of κa (κa = 156 instead of 94). This demonstrates the sensitivity of the particle size to the electrophoretic mobility at high zeta potential (predicted $|\zeta| \geq 160$ mV at pH>8) and a small value of κa.

Mobility measurements were also conducted in 10^{-4} M Na^+. To prepare a suspension, the buffer solutions shown in Table II-2 were diluted approximately five times with distilled water to achieve the desired Na^+ concentration. The Na^+ concentration was monitored using

the ion selective electrode as discussed. In addition, the measuring time was reduced to 2.5 minutes by acquiring only 32 waveforms instead of the usual 64 at a lower electric field of 170 Vm^{-1}. There was no noticeable widening of the wave spectrum during the measurement.

Results are shown in Figure II-8 and the measured and calculated mobilities with a = 0.9μm (solid line) are again compared. The $U(\zeta,\kappa a)$ relation computed using the program provided by O'Brien and White (2) showed no significant effect of the co-ion species in the buffer on the mobility at this experimental condition. Although both measurements and calculations show the presence of the maximum values in mobility, U^*_{max} at pH ≃ 5.5, the measured mobilities are consistently higher than calculated values. In particular, the theoretical U^*_{max} predicted by the computer solution (2) is 4.4 at this condition (κa = 30), but three measured U^* (U^* = 5.0, 5.3 and 4.9 at pH 5.0, 5.8 and 6.7, respectively) exceed this limitation.

(b) Moutray Crude-in-Water Emulsion. Measured mobilities for the Moutray crude-in-water emulsion in Na^+ concentrations of 10^{-3}, 10^{-2} and 10^{-1} M are shown by solid symbols as a function of pH in Figure II-9. The results were again analysed using the Ionizable Surface-Group model. As shown in Figure II-9, the electric properties of this crude oil can also be adequately explained with the model using a smaller value of $N_s = 5\times10^{17}$ m^{-2} (200 $Å^2$/site instead of 50 $Å^2$/site for bitumen), indicating a lower degree of surface coverage of carboxyl groups at the crude oil/water interface. This observation agrees with its lower acid number (a smaller amount of organic acid in the crude

oil) than for bitumen, as seen in Table II-1. Here, the most probable value of N_s was determined by minimizing the root mean square deviation of the measured U^* from calculated values as discussed in the previous paper (1).

5. Mobilities in $CaCl_2$ and $MgCl_2$ Solutions:

(a) Bitumen-in-Water Emulsion. The electrophoretic mobilities of the bitumen-in-water emulsion were also measured in aqueous $CaCl_2$ and $MgCl_2$ solutions. In Figure II-10, measured mobilities are shown as a function of the Ca^{++} concentration at pH 5.5 in the presence (circles) and absence (triangles) of 10^{-2} M NaCl. At this particular pH a buffer was not needed in the laser Doppler apparatus. The measured U^* in the presence and absence of 10^{-2} M NaCl are almost identical except those measured at the lowest Ca^{++} concentration of 10^{-4} M.

The measured U^* were first compared with the Ionizable Surface-Group model assuming that Ca^{++} as well as Na^+ are independent ions. The $U(\zeta,\kappa a)$ relation was always calculated using O'Brien and White's computer solution (2). The resultant U^* vs Ca^{++} concentration curve in the presence of 10^{-2} M NaCl (shown by the dashed line in Figure II-10) is consistently above that of the measured relation. This suggests the presence of a specific interaction between Ca^{++} and $RCOO^-$ on the bitumen surface. Simple mass action equations discussed by Pashley (11-13) were applied to describe the adsorption of Ca^{++} on the surface are:

$$RCOO^- + H^+ \rightleftharpoons RCOOH \qquad [3a]$$

$$RCOO^- + Ca^{++} \rightleftharpoons RCOOCa^+ \qquad [3b]$$

and the dissociation constants are defined by:

$$K_a = \frac{[RCOO^-]\ a_s(H^+)}{[RCOOH]} \qquad [4a]$$

$$K_{Ca} = \frac{[RCOO^-]\ [Ca^{++}]_s}{[RCOOCa^+]} \qquad [4b]$$

where the subscript 's' refers to the concentration of ions in solution immediately in contact with the bitumen surface. In addition, the Gouy-Chapman relation:

$$\left(\frac{d\psi}{dx}\right)^2 = \frac{2\ kT}{\epsilon} \sum_i n_i^o [\exp\ (-z_i \psi_o^*) - 1] \qquad [6a]$$

where

$$\psi_o^* = e\psi_o / kT \qquad [6b]$$

is integrated numerically up to x=0.6 nm (shear plane location) from the surface to calculate the zeta potential from the surface potential, ψ_o (1). Here n_i^o and z_i are the ion densities in the bulk solution and their valencies, respectively.

The values of pK_a and pK_{Ca} for acetic acid reported in the literature (17) are 4.5 and 0.53, respectively. Thus, the solid lines for the U^* versus Ca^{++} concentration relationships in Figure II-10 were calculated using these values both in the presence and absence of 10^{-2}

M NaCl. The U^* vs Ca^{++} relationships in the absence and presence of 10^{-2} M NaCl are identical for Ca^{++} concentrations above 10^{-3} M. However, the addition of NaCl results in larger values of U^* at lower Ca^{++} concentrations due to the smaller degree of the electrophoretic relaxation effect, even though it reduces the zeta potential (see Figure II-15). As demonstrated in Figure II-10, the measured and calculated U^* are now in good agreement.

Similar experiments were also conducted at three other pH of 4.0, 7.0 and 10 in the presence of 10^{-2} M Na^+ as shown in Figures II-11a and II-11b. The solution pH was adjusted using the buffer solutions as discussed previously. Again, the theoretical model appropriately predicts the measured U^* using the same value of pK_{Ca} of 0.53, except for some of the measured U^* in Ca^{++} concentrations below 10^{-3} M at pH 7.0 and 10.

Mobilities were also measured as a function of pH in 10^{-3} M $CaCl_2$ and $MgCl_2$. The experiments were conducted in the presence of two Na^+ concentrations of 10^{-3} and 10^{-2} M. Solid curves in Figure II-12a to II-12d are for theoretical U^* vs pH relationships using $pK_{Ca} = pK_{Mg} = 0.53$. As seen, the agreement between the measured and predicted U^* are reasonably good, though the measured U^* for both Ca^{++} and Mg^{++} rather abruptly exceed the predicted relationships at pH≥6.

(b) Moutray Crude-in-Water Emulsion. Measured U^* values for the Moutray crude emulsion in $CaCl_2$ solutions are shown as a function of pH in 10^{-3} M Ca^{++} and as a function of Ca^{++} concentration at pH 5.5 in Figures II-13a and II-13b, respectively. Both experiments were conducted in solutions containing 10^{-2} M Na^+. The measured and

theoretically predicted U^* using pK_{Ca}=0.53 are in good agreement, though some discrepancies again exist in Ca^{++} concentrations below 10^{-3} M at pH = 5.5 and 10.

(c) Mobility Measurements Without Buffer Solutions. Although there is no change in pH of the buffer solution in the presence and absence of 10^{-2} M $CaCl_2$ solution, the above observed discrepancies between the measured and predicted U^* in Ca^{++} and Mg^{++} below 10^{-3} M at pH>6 may be related to effects of the buffer solution during the measurement. Additional experiments were therefore conducted with the bitumen emulsions without the buffer solution. The pH of the solution was adjusted to 10 with NaOH and the Rank Brothers apparatus was used for the measurement. 10^{-2} M Na^+ was again present in the solution. Reductions of the measured mobilities from U^* = 4.6 to 4.1 and from U^* = 3.5 to 3.1 were observed in 10^{-4} and 10^{-3} M Ca^{++}, respectively. As shown by the solid symbols in Figure II-11, these new values lie on the theoretical line.

Mobilities of the heat treated carboxylated latex were also measured in the presence and absence of the buffer solution at pH 10 as a function of the Ca^{++} concentration in 10^{-2} M Na^+ as shown in Figure II-14. The preparation and characteristics of this latex will be described in a following chapter (this thesis chapter III). The U^* vs Ca^{++} relationships obtained using the laser Doppler apparatus in buffer

solution (open symbols) are above the theoretically predicted relationships, which were calculated using $N_s = 3.5 \times 10^{-18}$ m^{-2} (surface density of carboxyl groups for this latex), $pK_a = 4.5$, and $x = 0.6$ nm. In contrast, the solid symbols for mobilities measured using the Rank Brothers apparatus without buffer solution are on the theoretical line.

DISCUSSION

1. Laser Doppler Apparatus:

Recently Dalgleish et al., (6) reported that laser Doppler electrophoresis and particle microelectrophoresis give essentially identical mobilities for the casein-coated polystyrene latex particles. The pH of their solution was adjusted to 7.5 using 2×10^{-2} M imidazole buffer. Goff and Luner (5) measured mobilities of several latexes as a function of NaCl concentration over the range of 2×10^{-4} to 2×10^{-2} M using a laser Doppler apparatus very similar to our design. Their experiments were limited to a solution pH of 5.5. In fact, the mobility measurements using the laser Doppler apparatus have been mostly conducted either using buffer solutions of relatively high ionic strength (3,4,6,18-20) or without buffer at pH 5.5 (5). Therefore, the problem of pH drift has never been reported. The interaction of Ca^{++} and Mg^{++} with multivalent anions in the buffer solutions appears to be the main reason for observed discrepancies between measured and predicted U^* in low Ca^{++} and Mg^{++} concentrations at pH>6.

2. Estimation of ζ from U^* at Small Values of κa

The presence of Na^+ in the $CaCl_2$ and $MgCl_2$ solutions made the theoretical analysis somewhat difficult, especially for the estimation of ζ from ψ_0. Eq.[6] had to be integrated numerically. Experimentally however, it improved the accuracy of the zeta potential determination

from the measured mobility at certain experimental conditions. For example, curves 1 and 2 in Figure II-15 show the $U^*(\zeta,\kappa a)$ relationships for 3×10^{-4} M $CaCl_2$ in the presence and absence of 10^{-2} M NaCl. The mobility is much lower in the absence of NaCl at the same zeta potential due to the high degree of the electrophoretic relaxation effect. The measured U^* of 3.2±0.25 in the absence of NaCl corresponds to the zeta potential of any value between -61 and -103 mV as seen in Figure II-15. In contrast, the zeta potential was -60±4 mV for the measured U^* of 3.4±0.25 in the presence of 10^{-2} M Na^+. This exercise demonstrates that it is almost impossible to determine an accurate value of ζ from the measured mobility when measured $U^*\simeq U^*_{max}$.

According to O'Brien and White's computer solutions (2), U^*_{max} = 2.76 in 10^{-4} M $CaCl_2$ solution, whereas the measured U^* is 3.5 as shown in Figure II-10. Therefore, we observed measured mobilities larger than the theoretical limitation at two conditions: 10^{-4} M NaCl (Figure II-8) and 10^{-4} M $CaCl_2$ (κa = 30 and 51, respectively). Until this problem is properly understood, we should be very cautious of conducting electrophoresis measurements at $\kappa a<50$ and $|\zeta|>100$ mV, though it is often impossible to estimate the ζ value in advance.

3. Validity of pK_a and pK_{Ca} Values:

Although the measured and calculated mobilities in Ca^{++} and Mg^{++} solutions shown in Figures II-10 to II-13 are in good agreement, we are by no means claiming that Eqs. [3] and [4] with pK_a = 4.5 and pK_{Ca} = 0.53 accurately describe reactions occurring at the oil/water interface. More experimental evidence, especially a direct comparison

between the measured and calculated surface charge density and ion-exchange capacity, have to be conducted. However, these experiments were impossible to perform with our emulsions because of the coagulation of oil droplets at low pH and/or high electrolyte concentrations.

4. Application of Ion-binding Model to Enhanced Oil Recovery:

The main focus of this study was the development of an adequate theoretical model to successfully predict the electric properties of the oil/water interface over a wide range of brine concentrations, pH and temperatures, which would be encountered during enhanced oil recovery. In a previous paper (21), zeta potentials predicted from the model discussed here were used to generate a stability diagram for the bitumen-in-water emulsion as a function of NaCl and $CaCl_2$ concentrations for a wide range of pH. It was found that the results of coagulation experiments on the emulsion showed good agreement with the calculated stability diagram. The fact that the values of pK_a and pK_{Ca} for acetic acid in the bulk solution can be used encourages us to apply the present model to estimation of the flow behavior of emulsions in porous media during the steam injection process.

CONCLUSION

Although laser Doppler electrophoresis provides an accurate mobility measurement, the pH drift on the electrode surface is the biggest limitation when narrowly gapped electrodes are used. The Ionizable Surface-Group model adequately predicts the electric properties of bitumen and Moutray crude emulsions in mixed solutions of NaCl and $CaCl_2$ using pK_a and pK_{Ca} values for acetic acid in the bulk solution. The measured mobilities at $\kappa a < 60$ indicate that the accuracy of the theoretical $U(\zeta, \kappa a)$ relationship has to be re-examined. In the next chapter we will examine the U^*_{max} vs κa relationship over a range of κa between 8 and 300 in aqueous NaCl, $CaCl_2$ and $La(NO_3)_3$ solutions using a specially prepared high zeta potential latex.

TABLE II-1. Physical and Chemical Properties of Bitumen Extracted with Toluene from Athabasca Oil Sand, and Moutray Conventional Crude Oil used for Electrophoresis Measurements

Samples	Density[1] kgm^{-3}	Viscosity[1] mPa•s	Acid Number[2] mgKOH/g	Asphaltene[3] content, wt.%
Bitumen	1,010	400,000 2,000 (at 70°C)	2.0	17
Moutray Crude	838	5.23	0.26	0.18

[1] At 23°C.

[2] ASTM method D664.

[3] As in Bulmer, J.T., and Starr, J., "Syncrude Analytical Methods for Oil Sand and Bitumen Processing," Alberta Oil Sands Technology and Research Authority, Method 5.1, 1979.

TABLE II-2. Composition of Buffer Solutions Used for Laser Doppler Electrophoresis

pH range	Buffer composition	
3.0 - 5.5	$C_3H_4(OH)(COOH)_3$ 0.001 M	Na_2HPO_4 0.0005M
5.5 - 7.5	Na_2HPO_4 0.0005M	NaH_2PO_4 0.001 M
8.0 - 9.0	$Na_2B_4O_7$ 0.0005 M	HCl 0.001M
9.0 - 1.0.5	$Na_2B_4O_7$ 0.0005 M	NaOH 0.001M

TABLE II-3. Comparison of Electrophoretic Mobilities of Bitumen-in-Water Emulsions Measured by Particle Microelectrophoresis and Laser Doppler Electrophoresis

pH	Laser Doppler	Rank Brothers[1]	Predicted Values[2]
10^{-3} M NaCl			
3.9	3.5	4.0	3.5
7.0	6.1	6.0	6.4
9.0	6.3	6.5	6.5
10^{-2} M NaCl			
4.0	2.6	2.7	2.3
7.0	5.7	5.4	5.6
9.0	5.9	5.9	6.1

[1] In the absence of buffer.

[2] Mobilities predicted by the Ionizable Surface-Group model using $N_s=2\times10^{18}$ m^{-2}, $pK_a=4.5$ and $x=0.6$ nm.

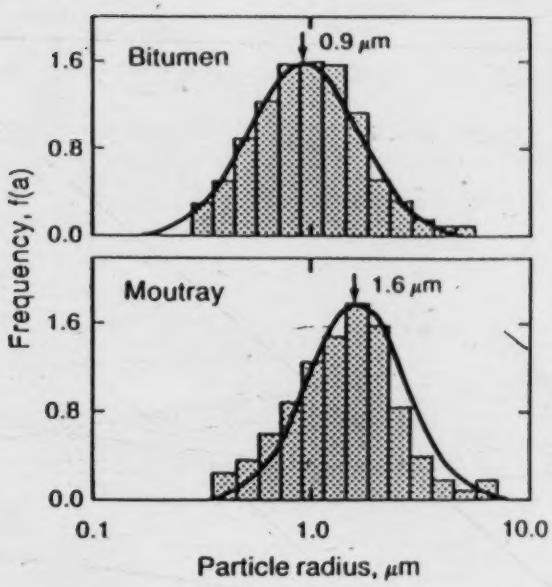

Figure II-1. Measured particle size distributions in histograms of bitumen-in-water and Moutray crude-in-water emulsions used for electrophoresis measurements. These distributions can be approximated, as shown by solid lines, using the log-normal distribution function:

$$f(a) = \frac{1}{\sigma\sqrt{2\pi}} \exp\left[0.5\left\{\frac{\ln(a)-\ln(\bar{a})}{\sigma}\right\}^2\right]$$

where σ=0.25 and $\bar{a}$=0.9 μm, and σ=0.22 and $\bar{a}$=1.6 μm for the bitumen and Moutray emulsions, respectively. σ and $\bar{a}$ are the standard deviation and mean value of the particle size distribution, respectively.

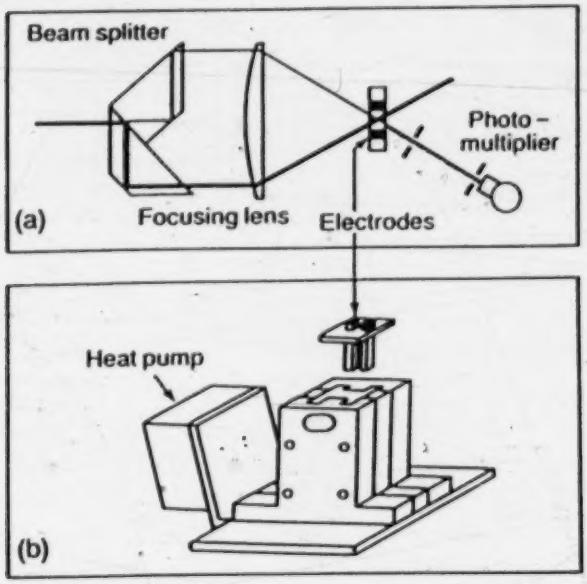

Figure II-2. Schematic diagram showing (a) the optical heterodyning and (b) temperature control systems of the laser Doppler apparatus. Main and reference beams from a beam splitter are focussed between a pair of platinized platinum electrodes (1.8 mm gap) placed in a cuvette (2 mm x 10 mm cross-section). A photomultiplier tube detects the beat developed by mixing the scattered light from the moving particles with the reference beam. The emulsion sample is placed in the cuvette which is held in an aluminum block. The temperature of this block is controlled using a solid state heat pump.

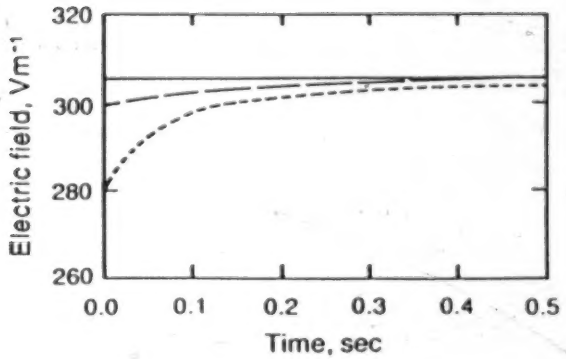

Figure II-3. Field strength of the electric field applied between the narrowly gapped electrodes as a function of time in 10^{-3} M (——), 10^{-2} M (— —) and 10^{-1} M (---) NaCl solutions. In the highest NaCl concentration of 10^{-1} M, approximately 0.2 seconds is required to obtain a constant field strength; thus the spectrum analyser was delayed 0.25 seconds before acquiring a Doppler signal.

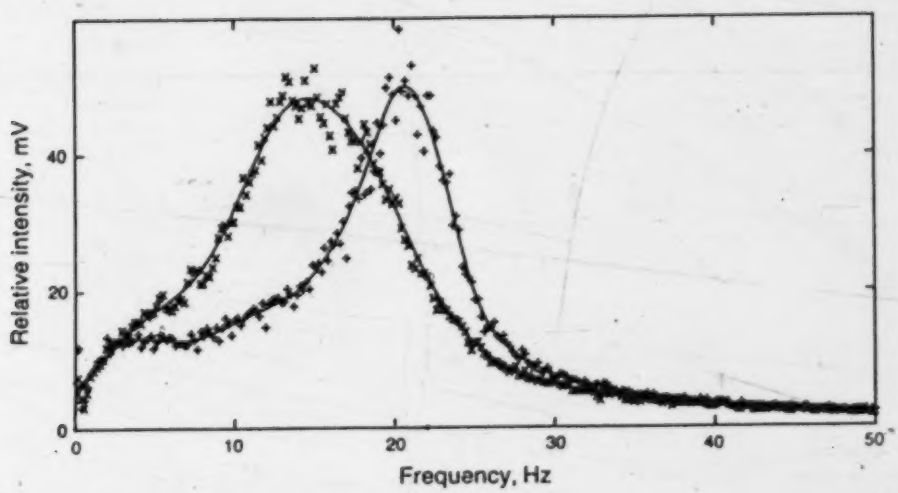

Figure II-4. Doppler spectra for bitumen emulsions in the absence (x) and presence (+) of buffer solution in 10^{-2} M NaCl at pH 9. The measured spectrum was curve fitted using a least square cubic spline method (solid lines), then numerically differentiated. The characteristic frequency shift, Δf, was calculated from the root of the differential equation. A Δf of 14.5 and 20.4 Hz in the absence and presence of buffer solution at an applied electric field of 445 Vm^{-1} corresponds to reduced mobilities of 4.5 and 5.9, respectively. The lower value of Δf and wider peak of the spectrum obtained in the absence of the buffer indicates the pH drift during the measurement.

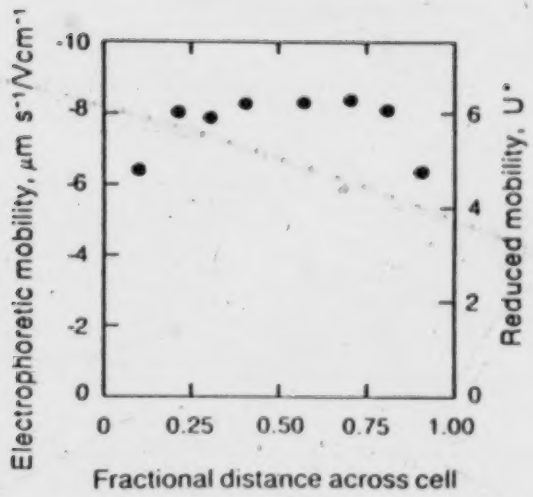

Figure II-5. Measured mobility profile of bitumen particles across the cell walls normal to the electric field in 10^{-2} M NaCl at pH 10. The measurement was conducted using the video recording technique as discussed in the Results section. The measured mobilities through the middle 60% of the cell are uniform.

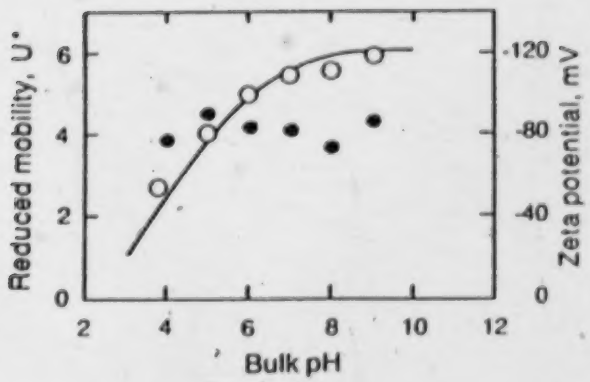

Figure II-6. Comparison of measured mobilities of the bitumen emulsion using a particle electrophoresis (○) and a laser Doppler (●) apparatus in 10^{-2} M NaCl. The line represents the U* vs pH relationship predicted by the Ionizable Surface-Group model. The mobilities measured using the particle electrophoresis apparatus agree with the predicted relationship while those measured using the laser Doppler apparatus show almost no change in mobility for $4<pH<9$. The values of zeta potentials indicated are applicable only at $\kappa a>300$.

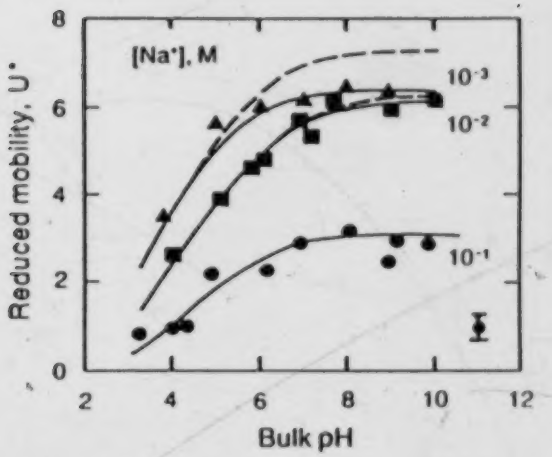

Figure II-7. Measured (symbols) and calculated (curves) mobilities for the bitumen emulsion as a function of pH in 10^{-3}, 10^{-2} and 10^{-1} M NaCl. The mobilities were calculated for a=0.9 (solid curves) and 1.5 μm (dashed curves). The importance of particle size on the mobility, due to different degrees of the electrophoretic relaxation effect, can be seen at high pH in 10^{-3} M NaCl. The error bar at the lower right indicates the estimated reproducibility of the measured mobility.

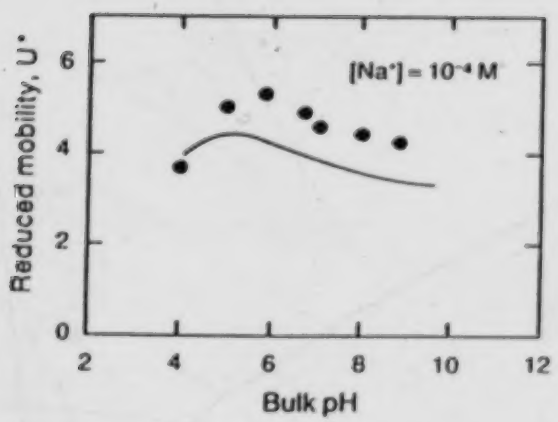

Figure II-8. Same as Figure II-7 but in 10^{-4} M NaCl. Although the measured mobilities show the presence of the maximum, U^*_{max}, three measured mobilities (U^*=5.0, 5.3 and 4.9 at pH 5.0, 5.6 and 6.7, respectively) exceed the theoretical U^*_{max} of 4.4 at κa=30.

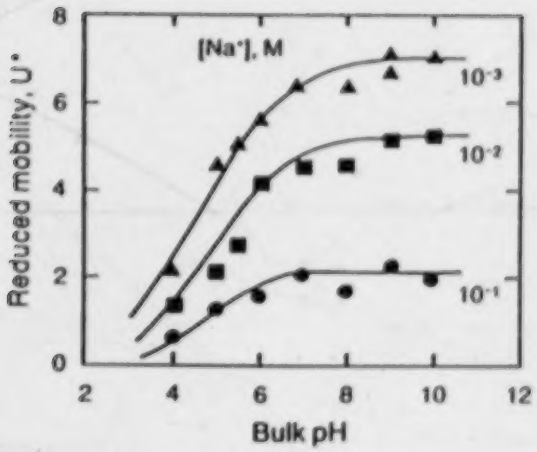

Figure II-9. Same as Figure II-7 but for the Moutray crude emulsion. Theoretical mobilities were calculated using $N_s=5\times10^{17}$ m^{-2}, $pK_a=4.5$, x=0.6 nm and a=1.6 μm.

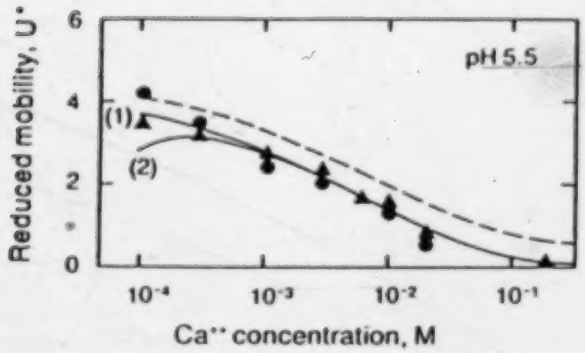

Figure II-10. Measured (symbols) and calculated (curves) mobilities of the bitumen emulsion in the absence (▲) and presence (●) of 10^{-2} M NaCl as a function of Ca^{++} concentration at pH 5.5. See text for difference between the solid and dashed curves. In the absence and presence of 10^{-2} M NaCl the curves are identical for Ca^{++} concentrations above 10^{-3} M. The presence of NaCl increases the mobility at lower concentrations by reducing the electrophoretic relaxation.

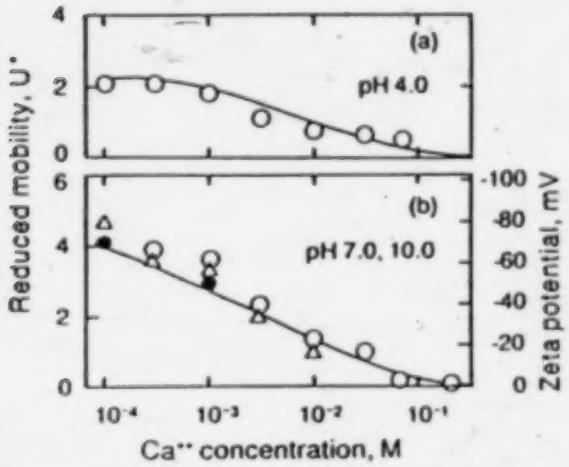

Figure II-11. Same as Figure II-10 but (a) at pH 4 (o), and (b) at pH 7 (Δ) and pH 10 (o). Solid circles in 10^{-3} and 10^{-4} M Ca^{++} were obtained without buffer solution using the Rank Brothers particle electrophoresis apparatus. For details, see text. The values of zeta potentials indicated are applicable only at $\kappa a > 300$.

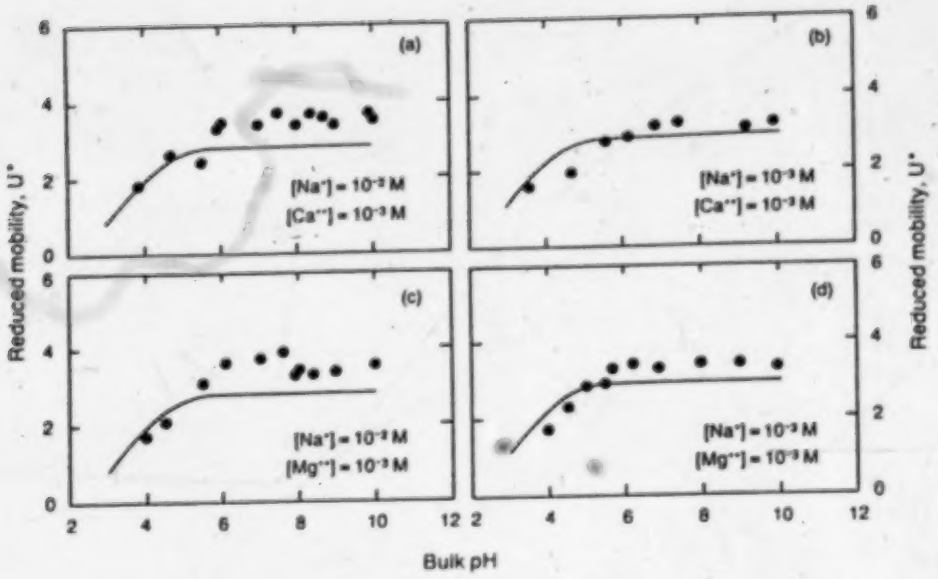

Figure II-12. Measured and calculated mobilities of the bitumen emulsion as a function of pH in 10^{-3} M Ca^{++} and Mg^{++} concentrations in the presence of 10^{-3} M and 10^{-2} M Na^{+}. The discrepancies between the measured and predicted U^{*} vs pH at pH>6 are discussed in the text.

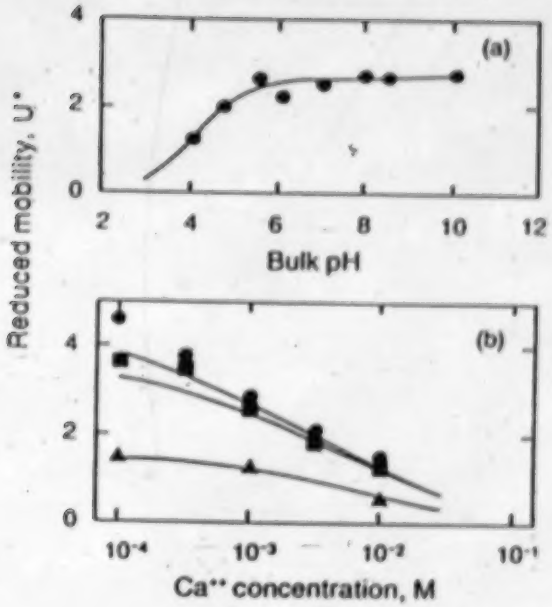

Figure II-13. Measured and calculated mobilities of the Moutray crude emulsion (a) as a function of pH in 10^{-3} M Ca^{++} and (b) as a function of Ca^{++} concentration at pH 4.0 (▲), 5.5 (■) and 10 (●). Measurements were conducted in the presence of 10^{-2} M Na^{+}.

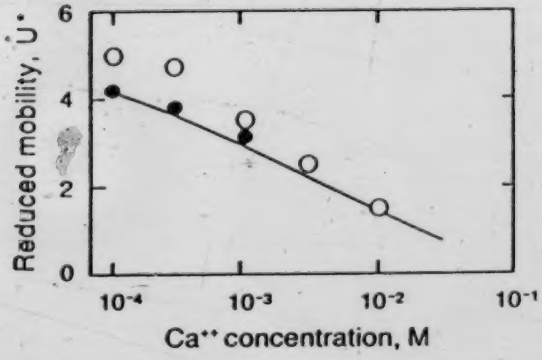

Figure II-14. Measured mobilities of the heat treated carboxylated latex particles with (o) and without (•) buffer solutions as a function of Ca^{++} concentration using the laser Doppler and Rank Brothers apparatuses, respectively, at pH 10. The line represents the theoretical U^* vs Ca^{++} relationships calculated using $N_s=3.5\times10^{18}$, $pK_a=4.5$, $pK_{Ca}=0.53$ and x=0.6 nm (18).

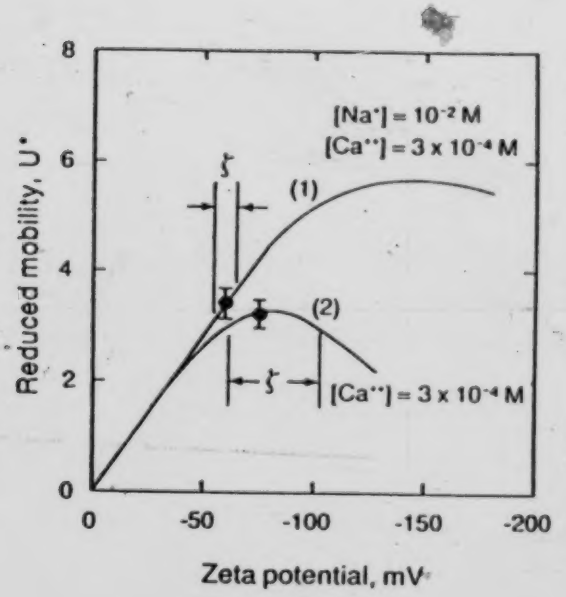

Figure II-15. Theoretical $U^*(\zeta,\kappa a)$ relationship (2) for the bitumen emulsion in 3×10^{-4} M Ca^{++} in the presence (curve 1) and absence (curve 2) of 10^{-2} M Na^+. The measured $U^*=3.2\pm0.25$ in the absence of Na^+ corresponds to $-103<\zeta<-61$ mV. In contrast, $\zeta=-60\pm4$ mV for $U^*=3.4\pm0.25$ in the presence of 10^{-2} M Na^+. Thus, the addition of Na^+ in the solution significantly improves the ζ determination from the measured U^* at $U^*\simeq U^*_{max}$.

REFERENCES

1. Takamura, K., and Chow, R.S., Colloids and Surfaces **15**, 35 (1985).

2. O'Brien, R.W., and White, L.R., J. Chem. Soc. Faraday Trans. 2, **74**, 1607 (1978).

3. Ware, B.R., Adv. Colloid Interface Sci. **4**, 1 (1974).

4. Uzgiris, E., Adv. Colloid Interface Sci. **14**, 75 (1981).

5. Goff, J.R., and Luner, P., J. Colloid Interface Sci. **99**, 468 (1984).

6. Dalgleish, D.G., Dickinson, E., and Whyman, R.H., J. Colloid Interface Sci. **108**, 174 (1985).

7. Melrose, J.C., Soc. Pet. Eng., 57th Ann. Conf., New Orleans, SPE 10971 (1982).

8. Takamura, K., and Chow, R.S., J. Can. Petrol. Tech. **22**, 22 (1983).

9. Soo, H., and Radke, C.J., J. Colloid Interface Sci. **102**, 462 (1984).

10. Morrow, N.R., Lim, H.T., and Ward, J.S., SPE Formation Evaluation, February, 89 (1986).

11. Pashley, R.M., J. Colloid Interface Sci. **83**, 531 (1981).

12. Pashley, R.M., and Quirk, J.P., Colloids and Surfaces **9**, 1 (1984).

13. Pashley, R.M., Clay and Clay Minerals **33**, 193 (1985).

14. Uzgiris, E., and Kaplan, J., Rev. Sci. Instrum. **45**, 120 (1974).

15. Tamamushi, R., and Takahashi, K., Electroannal. Chem. Interface Electrochem. **50**, 277 (1974).

16. Ohshima, H., Healy, T.W., and White, L.R., J. Chem. Soc. Faraday Trans. 2, **79**, 1613 (1983).

17. Martell, A.E., and Smith, R.M., "Critical Stability Constants, Vol. 3: Other Organic Ligands," Plenum, New York, 1979.

18. Smith, B.A., Ware, B.R., and Weiner, R.S., Proc. Natl. Acad. Sci. USA 73, 2388 (1976).

19. Uzgiris, E.E., and Kaplan, J.H., J. Colloid Interface Sci. 55, 148 (1976).

20. Wilcoxon, J.P., and Schurr, J.M., J. Chem. Phys. 78, 3354 (1983).

21. Takamura, K., Chow, R.S., and Tse, D.L., Proc. Symp. on Flocculation in Biotechnology and Separation Systems, San Francisco, California, July, 1986.

CHAPTER III

EFFECTS OF INNER DOUBLE LAYER STRUCTURE ON THE ELECTROKINETIC POTENTIAL OF LATEX PARTICLES*

* A version of this chapter has been submitted for publication. Chow, R.S. and Takamura, K., Journal of Colloid and Interface Science, 1987.

INTRODUCTION

In two previous papers (1,this thesis chapter II) the electrophoretic mobilities of bitumen and Moutray conventional crude oil emulsions were studied over a wide range of pH and electrolyte concentrations. The analysis of measured results for both the bitumen and Moutray emulsions using the Ionizable Surface-Group model indicated that the negative charge of the crude oil/water interface is due to the dissociation of carboxyl groups present at the interface. It also demonstrated that zeta potentials, ζ, calculated from the measured mobilities were in good agreement with theoretical predictions when the shear plane was assumed to be located 0.6 nm from the particle surface. The location of the shear plane was independent of the NaCl, $CaCl_2$ and $MgCl_2$ concentrations.

In contrast, Healy and White (2) and Harding and Healy (3) used a much larger value of 2 nm for the location of the shear plane to explain ζ for mineral oxides and latex particles. This discrepancy in the shear plane location used for ζ calculations arises from the fact that crude oil emulsions have significantly larger values of $|\zeta|$ than metal oxides or latex: e.g., $|\zeta| \simeq 100$ mV for bitumen vs $|\zeta| < 60$ mV for latex (3,4) and silica (5) in 10^{-2} M NaCl at pH>8. In addition, a value of $d|\zeta|/d\log C = -60$ mV (where C is the concentration of the monovalent electrolyte) predicted from the Gouy-Chapman theory with a constant diffuse layer charge is obtained for bitumen and Moutray crude oil emulsions at high pH, whereas the usual value observed experimentally for many solid particles is only -(20-30 mV) (6).

Large negative values of ζ for hydrocarbon droplets in aqueous electrolyte solutions above neutral pH have long been reported (7-12). Wiersema et al (13) discussed some of these results to test their theory for the electrophoretic relaxation effect. Reasons for the failure of the Ionizable Surface-Group model for predicting the observed small value of $d|\zeta|/d\log C$ have not been well understood (2,6). Some explanations offered for latex particles are effects of the hairy surface, counter-ion, and co-ion adsorption, or ion exchange across the shear plane as discussed by Goff and Luner (14).

These results appear to suggest that the liquid/liquid interface has significantly larger electrokinetic potentials than the solid/water interface. To investigate this difference, we measured electrophoretic mobilities of carboxylated latex particles. This particular latex was chosen because it has a similar density of carboxyl groups and particle size as the bitumen emulsions studied in the previous paper (this thesis chapter II). The results show that large negative values of ζ, similar to those of the bitumen emulsions, are obtained only when the latex particles are treated at above the glass transition temperature of the polymer, thus suggesting that the surface roughness or "hairiness" of the latex particles may be the main reason for the reported small zeta potentials. Mobilities larger than the theoretical maximum mobilities predicted by O'Brien and White's computer solution (15) were observed using the heat treated latex at $8<\kappa a<80$ in NaCl, $CaCl_2$ and $La(NO_3)_3$ solutions, where κ is the reciprocal Debye-Huckel length and a is the particle radius.

EXPERIMENTS

1. Latex Particles

A surfactant free, carboxylated styrene-acrylamide copolymer latex was used. As described by Kawaguchi (16), carboxyl groups on this latex are the result of the hydrolysis of amide groups on the surface with a concentrated NaOH solution. The surface density of the carboxyl groups, N_s, and the particle radius, a, are 3.53×10^{18} m^{-2} and 805 nm, respectively ($a_s/a_n = 1.0014$, where a_s and a_n are the surface averaged and number averaged radii, respectively).

The latex was heat treated by placing 6 ml of the original suspension, which was 14.5% in solid, into an autoclave (22 mm diameter and 30 mm deep) that was fitted with a teflon liner. The autoclave was then placed in an oven set at 115 °C for 16 hours. During the heat treatment nearly one-third of the latex particles were coagulated and formed a solid mass at the bottom of the autoclave.

2. Electrophoresis

A laser Doppler apparatus described in a previous chapter (this thesis chapter II) was used to measure electrophoretic mobilities of the original and heat treated latexes in 10^{-3}, 10^{-2} and 10^{-1} M NaCl solutions at 25 °C. Dilute buffer solutions were used to prevent pH drift from occurring on the electrode surfaces. Deionized water (Milli-Q water system, Millipore Ltd., Mississauga, Ontario) was used

for all measurements. This water had an electrical conductance of 11 nSm^{-1} and pH of 5.5 when it was saturated with CO_2 from air. A Doppler spectrum for the latex measured in a 10^{-2} M NaCl solution at pH 10 is shown in Figure III-1a.

For measurements in NaCl concentrations below 10^{-3} M, and also in $CaCl_2$ and $La(NO_3)_3$ solutions, a Rank Brothers particle electrophoresis apparatus was used. Although the latex particles were negatively charged at all the conditions studied, mobility is reported in the absolute value of the reduced electrophoretic mobility, U^*, which is given by;

$$U^* = \frac{3e\eta|U|}{2\epsilon kT} \qquad [1]$$

where 'e' is the electron charge, η and ϵ are the viscosity and permittivity of water, respectively, k is the Boltzmann constant, and T is the absolute temperature.

RESULTS

1. U^* for Original Latex in NaCl Solution

Figure III-2a shows measured U^* for the original latex as a function of pH in 10^{-3}, 10^{-2} and 10^{-1} M NaCl. The U^* vs pH relationships are similar to the results for carboxylated latex reported by Ottewill and Shaw [latex D in ref.(4)], which are reproduced in Figure III-3 for comparison. However, the U^* values are significantly smaller than for bitumen emulsions [e.g. U^* = 6.4, 5.9 and 3.2 in 10^{-3}, 10^{-2} and 10^{-1} M at pH>8 (this thesis chapter II)] at the same pH and electrolyte concentrations.

The Ionizable Surface-Group model using the Gouy-Chapman theory (1,3,this thesis chapter II) was applied to explain the measured results using material constants of N_s = 3.53 x 10^{18} and pK_a = 4.5, where pK_a is the dissociation constant of the carboxyl groups. First, the location of the shear plane, x, was assumed to be a single value of 2 nm as from Harding and Healy (2), and the $U^*(\zeta, \kappa a)$ relationship was obtained using the formula of Ohshima et al. (17). κ is the reciprocal Debye-Huckel length, which is given by;

$$\kappa = [e^2 \Sigma n_i z_i^2 / \epsilon kT]^{1/2} \qquad [2]$$

where n_i and z_i are the density and valency of ionic species i, respectively. Results of the theoretical U^* vs pH relationships are shown by dashed lines in Figure III-2a. As seen, the agreement between

the predicted and measured U^* is reasonable only in 10^{-2} M NaCl, while the theoretically predicted U^* vs pH relationships are lower in 10^{-1} M and higher in 10^{-3} M than observed experimentally. Careful inspection of results for amphoteric latex reported by Harding and Healy (3) showed a similar discrepancy between theoretically predicted and measured mobilities in 10^{-1} M NaCl.

The experimental results were then analysed by varying the value of x, the shear plane location. As shown by solid lines in Figure III-2a, the best fit to the experimental results is obtained when x = 4.3, 1.9, and 0.8nm for 10^{-3}, 10^{-2} and 10^{-1} M NaCl solutions, respectively. The same analysis was applied to the amphoteric (3) and carboxylated latexes (4), and the values of x which resulted in the best fit to the measured mobilities are listed in columns 2 and 3 of Table III-1.

The results in Table III-1 show that for three latexes, larger values of x are needed to explain the measured mobility for lower electrolyte concentrations, and vice versa. This observation may suggest that the latex surface is not smooth, but rather is covered by polymer chains (hairs) which have charged groups at the ends. As the electrolyte concentration decreases, the polymer chains expand toward the bulk solution resulting in an increase in the value of x. This hypothesis was tested using a heat treated latex.

2. U^* for Heat Treated Latex in NaCl Solution

If the large value of x needed to explain the measured U^* for the latex is due to the surface roughness (or hairiness), and if the latex

will have a smoother surface when the suspension is heated above the glass transition temperature of polystyrene, T_g = 100°C (18), such heat treatment would increase the mobility of the original latex. This was indeed the case. The Doppler spectrum shown in Figure III-1b was obtained by mixing both the original and heat treated latexes in 10^{-2} M NaCl at pH 10 with an applied electric field of 480 Vm^{-1}. Two peaks of 11.8 and 22.6 Hz (U^* = 3.2 and 5.9) which correspond to the original and heat treated latexes, respectively, can be clearly seen. The heat treatment nearly doubled the measured U^* at this condition.

Electrophoretic mobilities of the heat treated latex particles were then determined as a function of pH in 10^{-4}, 10^{-3}, 10^{-2} and 10^{-1} M NaCl solutions. The symbols in Figure III-2b represent the measured U^*, and lines represent the U^* vs pH relationships predicted by the Ionizable Surface-Group model. The calculations used the same values of N_s and pK_a as the original latex, but only a single value of x = 0.6 nm which is the same as used for the bitumen and Moutray crude oil emulsions (this thesis chapter II). The values of measured U^* for the heat treated latex were significantly larger than for the original latex at the same NaCl concentration and pH, and the U^* vs pH relationships were adequately explained by the theoretical model, except that obtained for the lowest NaCl concentration of 10^{-4} M (κa = 26). As observed with the bitumen emulsion at κa = 30 (this thesis chapter II), the measured U^* exceeded the theoretical maximum value, U^*_{max}, of 4.4 predicted by the computer solution of O'Brien and White (15) at pH$\geq$5. Therefore, we observed measured mobilities larger than the theoretical limitations using both the bitumen emulsion and the heat treated latex particles at κa = 30 and 26, respectively.

3. U^*_{max} vs κa at $8<\kappa a<80$

A series of experiments were performed to investigate the discrepancies between the observed and theoretically predicted U^*_{max}. U^* was measured as a function of κa at pH 5.5 in the presence of mono- and di-valent counterions. Mobility was measured using the Rank Brothers particle electrophoresis apparatus without the buffer solution. The exact experimental conditions are listed in Table III-2 together with the values of κa, ζ predicted from the Ionizable Surface-Group model, measured U^*, theoretically predicted U^*_{max} and $\zeta(U^*_{max})$. $\zeta(U^*_{max})$ is the value of ζ corresponding to the U^*_{max} as predicted from the $U^*(\zeta, \kappa a)$ relation (15). Values of ζ in $CaCl_2$ solutions were predicted using $pK_{Ca} = 0.53$ (this thesis chapter II). To ensure the accuracy of the electrolyte concentration, the specific conductance was measured for each suspension. The measured values are in good agreement with the theoretical values except for the solution with the lowest NaCl concentration of 1.0×10^{-5} M, which had a value 10% larger than expected. The measurement in 1×10^{-3} M NaCl was conducted at pH 8.

As seen in Table III-2, most of the measurements were conducted at the condition of $|\zeta|>|\zeta(U^*_{max})|$. Although the measured U^* values decreased with reducing κa values as predicted from theory (15), they were consistently larger than predicted U^*_{max}. Experiments were also conducted in $La(NO_3^-)_3$ solutions between 1.6×10^{-6} and 2.6×10^{-5} M, and the κ values were calculated without considering the hydrolysis of La^{+++}, though significant amounts of $La(OH)^{++}$ and $La(OH)_2^+$ are present at the

experimental condition of pH 5.5. Thus, the real values of κa are somewhat smaller. We are not, at this point, able to predict ζ in $La(NO_3)_3$ solutions; thus the condition of $|\zeta| \geq |\zeta(U^*_{max})|$ may not be attained. Nonetheless, the measured U^* values were again larger than the predicted U^*_{max} except in 2.5×10^{-5} M $La(NO_3)_3$ solution. The results shown in Table III-2 consistently demonstrate that discrepancies between the measured U^* and the predicted U^*_{max} increase with the reduction of κa values for all the counterions studied.

DISCUSSION

1. Location of the Shear Plane

As seen in Table III-2 for the results of the heat treated latex, and the bitumen and Moutray crude oil emulsions, we now have strong evidence which suggests that the shear plane is located 0.6 nm from the smooth surface. This value is independent of NaCl and $CaCl_2$ concentrations from 10^{-4} to 10^{-1} M, and pH from 3 to 11, and is applicable to the estimated surface potential as high as 300 mV [see Figure 4 in ref.(1)]. Stigter (19) and Israelachvili (20) demonstrated that water between two clay mineral surfaces maintains its bulk properties except one layer of molecules at each surface. Stigter (19) also showed from the analysis of diffusion and electrokinetic measurement data that the shear plane for dodecyl sulfate micelles is at 0.1 nm from the hydrated sulfate group of 0.43 nm, thus located approximately 0.5 nm from the hydrocarbon core. His analysis also explains our observed value of 0.6 nm.

Although values of x listed in Table III-1 for the original, amphoteric and carboxyl latexes can be used to fit the experimental results adequately, these values are not representative of the real location of the shear plane. The Ionizable Surface-Group model used in this study assumes that the surface groups are located on an imaginary plane of no thickness. If they are distributed within a layer of finite thickness, the theory does not appropriately describe their dissociation behavior. The method discussed by Ohshima et al. (21) for

the description of the potential distribution across the surface charge layer has to be incorporated in the present model.

As mentioned before, small ζ values observed for latex and mineral oxide particles are most often explained by the specific adsorption of counterions (counterion binding) on the surface (22-27). The results of the original and heat treated latexes in this study suggest that some of those results should be re-analysed.

2. Observations of Measured $U^* > U^*_{max}$

Although electrokinetic theories for spherical particles have been extensively studied (13,15, 30-32), the validity of these theories has seldom been investigated experimentally. Ottewill and Shaw (4) measured the electrophoretic mobilities of five different latexes ranging in diameter from 60 to 420 nm. The measured U^* vs κa at $1<\kappa a<100$ in NaCl solutions were in good agreement with the theoretical curves [Figure 7 in ref. (4)]. However, their studies were limited to $|\zeta| < |\zeta(U^*_{max})|$, according to our calculations using the values of x listed in Table III-1. At the same time, their results obtained in $Ba(NO_3)_2$ were often above the theoretically predicted U^*_{max} [Figure 8 in ref. (4)].

The results of the measured U^* and theoretically predicted U^*_{max} vs κa relationships for the heat treated latex shown in Table III-2 are plotted in Figure III-4. In the figure, values for bitumen emulsions in NaCl and $CaCl_2$ solutions (this thesis chapter II), results by Ottewill and Shaw (4) for a carboxylated latex in $Ba(NO_3)_2$ (Latex E,

which had the highest charge density among five latexes studied), and for silver iodide in 1.2×10^{-2} M KNO_3 ($\kappa a = 11$) (33) are also included. These additional data points are in good agreement with the U^* vs κa relationships obtained using the heat treated latex. The measured results in the presence of divalent counterions suggest that a minimum in the U^*_{max} vs κa relation occurs at $\kappa a \simeq 40$, instead of the theoretical prediction at $\kappa a \simeq 4$.

Although the measured U^* approach the theoretical U^*_{max} relationships at $\kappa a > 80$ for all three electrolytes, this observation does not necessarily mean that the theory is applicable at that condition. As seen in column 3 in Table III-2, the ζ potential of the latex particles decreases with increasing electrolyte concentration, and becomes $|\zeta| \leq |\zeta(U^*_{max})|$ at $\kappa a > 60$-70 in NaCl and $CaCl_2$ solutions for our latex. Additional experiments using a different particle size are necessary to make definite conclusions.

Since we can estimate the ζ potential, it is possible to determine the experimental $U^*(\zeta, \kappa a)$ relationship. This is shown in Figure III-5a for an NaCl solution at $26 < \kappa a < 30$. Solid symbols represent the measured U^* vs estimated ζ relationships for a bitumen emulsion (a = 900 nm) (this thesis chapter II) and the heat treated latex (a = 805 nm) in 10^{-4} M NaCl. The solid lines are from O'Brien and White's computer solutions for κa = 26 and 30, respectively. The maximum in the measured mobility is 5.2 at $\zeta \simeq -150$ mV instead of the theoretically predicted value of 4.2-4.4 at $\zeta \simeq -135$ mV. The measured U^* are consistently larger than predictions at $|\zeta| > 100$ mV.

Similarly, Figure III-5b illustrates the U^* vs ζ relationships for

κa = 36 in 10^{-4} M NaCl solution in the presence of 3.0×10^{-5} M $CaCl_2$. The solid line is again from the computer solution and symbols represent the heat treated latex measured at $3.5 < pH < 7$. The addition of 3.0×10^{-5} M $CaCl_2$ significantly reduces $|\zeta|$ for the latex from ~200 mV to ~100 mV at pH 7 due to the binding of Ca^{++} with $RCOO^-$ on the surface as described in a previous chapter (this thesis chapter II). The presence of divalent counterions in the double layer also increases the electrophoretic relaxation effect, thus reducing the predicted U^* to compare to the relationships shown in Figure III-5a. The measured mobilities are again larger than the predicted values. The experimental conditions as well as the results shown in Figures III-5a and III-5b are also summarized in Tables III-3 and III-4.

The experimental results described above strongly suggest that the computer solution for the $U^*(\zeta, \kappa a)$ relationship (15) overestimates the electrophoretic relaxation effect at $\kappa a < 100$. The same theory has been extended to describe other electrokinetic phenomena, such as dielectric relaxation (34), electric conductance (17, 35, 36), and the sedimentation potential (37) of colloidal dispersions, etc. Zukoski and Saville (38) observed that the ζ potentials for the same latex calculated from the measured electrophoretic mobility and suspension conductivity are substantially different. Various electrokinetic theories should be tested using the heat treated latex described in this paper to improve our understanding of the electrokinetic phenomena.

TABLE III-1. List of Shear Plane Locations which Result in the Best Fit to Experimentally Observed U* vs pH Relationships in Aqueous NaCl Solutions

NaCl Concentration, M	Amphoteric Latex[1]	Carboxylated Latex[2]	Original Latex	Heat Treated Latex	Bitumen[3]
10^{-1}	1.2	-	0.8	0.6	0.6
5.0×10^{-2}	-	1.2	-	-	-
10^{-2}	2.0	2.0	1.9	0.6	0.6
10^{-3}	2.0	-	4.3	0.6	0.6
5.0×10^{-4}	-	3.6	-	-	-

[1,2] Measurements reported in (3) and (4) respectively.

[3] As in ref. (1).

TABLE III-2. Measured Mobilities of the Heat Treated Latex at Bulk pH of 5.5 in NaCl, $CaCl_2$ and $La(NO_3)_3$ Solutions, and the Predicted Maximum Mobilities U^*_{max}

Electrolyte Concentration, M	κa	ζ[1] mV	U^* measured	U^*_{max}[2] calculated	$\zeta(U^*_{max})$[3] mV
NaCl					
1.0×10^{-5}	8.3	-166	4.3	3.2	-111
2.0×10^{-5}	12	-169	4.8	3.4	-113
6.0×10^{-5}	20	-155	5.2	3.9	-115
9.0×10^{-5}	25	-149	5.1	4.1	-115
1.0×10^{-4}	26	-151	5.2	4.2	-136
2.0×10^{-4}	37	-141	5.6	4.6	-138
4.0×10^{-4}	53	-131	5.8	5.1	-139
6.0×10^{-4}	65	-126	5.8	5.4	-139
1.0×10^{-3}	83	-162	6.3[4]	5.8	-140
$CaCl_2$					
3.6×10^{-6}	8.7	-121	2.7	1.7	-58.4
1.2×10^{-5}	16	-109	2.6	1.9	-61.3
3.8×10^{-5}	28	-94.8	2.6	2.3	-62.9
5.7×10^{-5}	35	-89.8	2.6	2.4	-63.4
3.1×10^{-4}	80	-69.2	3.2	3.1	-81.7
$La(NO_3)_3$					
1.6×10^{-6}	8.2		1.9	1.1	-37.6
5.2×10^{-6}	15		1.6	1.3	-39.4
1.8×10^{-5}	27		1.6	1.5	-41.0
2.6×10^{-5}	33		1.6	1.6	-52.5

[1] ζ predicted from the Ionizable Surface-Group model using $N_s=3.5\times10^{18}$ m^{-2}, pKa=4.5 and x=0.6 nm.

[2] Maximum mobilities predicted from O'Brien and White's computer solution (15).

[3] ζ corresponding to U^*_{max} as predicted from the computer solution.

[4] Measured at pH=8.

TABLE III-3. Measured Mobilities of Bitumen and Heat Treated Latex in 10^{-4} M Na^+ (κa=26 and 30, respectively)

Solution pH	U^* measured	ζ^1 mV	U^{*2} expected
	Heat Treated Latex		
4.0	3.8	-101	4.1
5.0	4.8	-134	4.2
5.5	5.3	-150	4.1
6.0	5.2	-166	3.9
7.0	5.1	-191	3.6
7.8	4.8	-209	3.4
9.0	5.0	-225	3.2
	Bitumen[3]		
4.0	3.7	-92	4.0
5.0	5.0	-122	4.4
5.8	5.3	-149	4.3
6.7	4.9	-176	4.0
7.0	4.6	-185	3.8
8.0	4.4	-204	3.6
8.8	4.3	-215	3.4

[1,2] See Table 2.

[3] Results reported in this thesis chapter II.

TABLE III-4. Measured Mobilities of Heat Treated Latex in 10^{-4} M NaCl in the Presence of 3.0×10^{-5} M $CaCl_2$ at 3.5<pH<7.0 (κa=36)

Solution pH	U^* measured	ζ^1 mV	U^{*2} expected
4.0	3.1	-75	2.8
4.5	3.2	-85	2.8
5.0	3.1	-93	2.8
7.0	3.0	-100	2.7

[1,2] See Table 2.

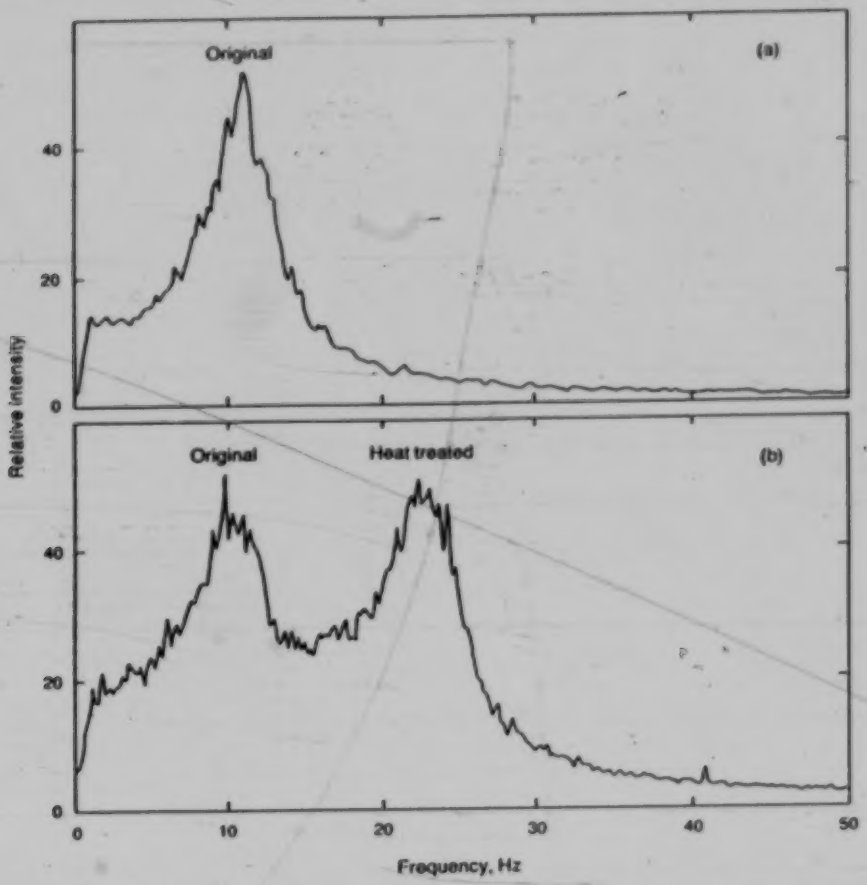

Figure III-1. (a) Doppler spectrum for a carboxylated polystyrene-acrylamide latex in 10^{-2} M NaCl solution at pH 10. The measured frequency shift of 11.8 Hz at the applied electric field of 480 Vm^{-1} corresponds to the reduced mobility, U^*, of 3.2.

(b) Spectrum for a mixture of the original and heat treated latexes measured at the same conditions. The heat treatment nearly doubled the frequency shift to 22.6 Hz (U^*=5.9) at this condition.

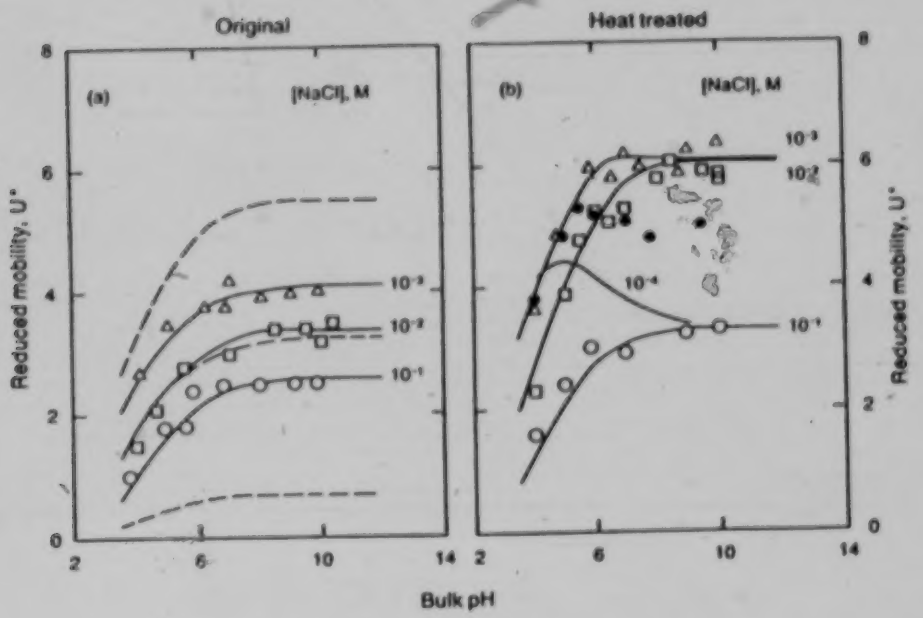

Figure III-2. (a) Measured (symbols) and calculated (solid and dashed lines) electrophoretic mobilities of the original latex as a function of pH in aqueous NaCl solutions of (Δ):10^{-3} M, (□):10^{-2} M and (o):10^{-1} M. The dashed lines were calculated assuming that the shear plane is at 2.0 nm from the surface, and the solid lines were calculated using values of x as listed in Table III-1.

(b) Same as (a) but for the heat treated latex. Measurements were also conducted in (●):10^{-4} M NaCl solution. The solid lines were calculated using a single value of x=0.6 nm, and adequately explain the measured U* vs pH relationships except that measured in 10^{-4} M NaCl.

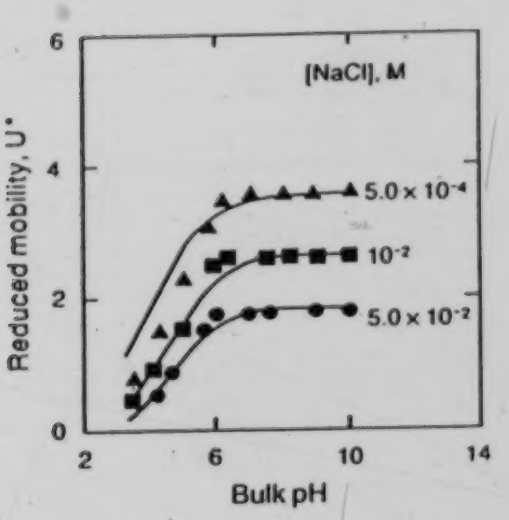

Figure III-3. Measured mobilities (symbols) of carboxylated latex particles in aqueous NaCl solutions reported by Ottewill and Shaw (4), and theoretical predictions (solid lines) using $N_s=5.08\times10^{17}$ m^{-2}, $pK_a=4.5$ and values of x as listed in Table 1.

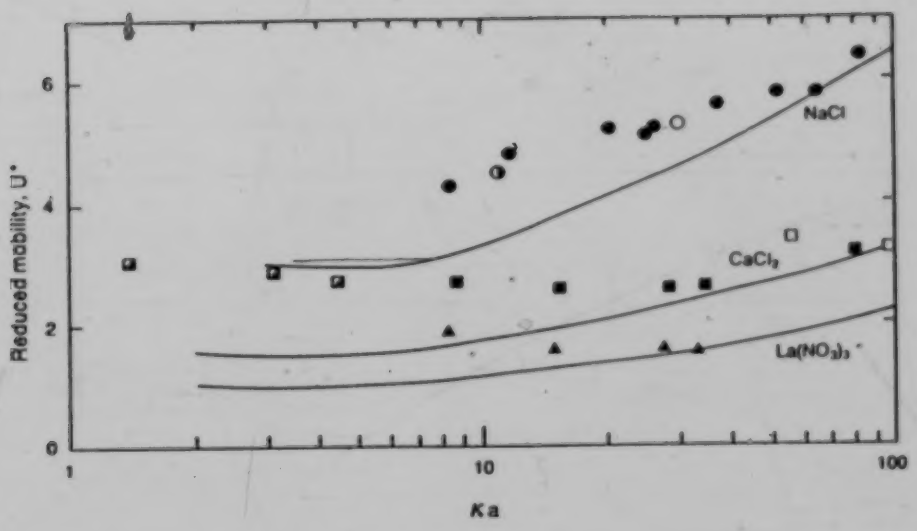

Figure III-4. Plot of experimental results of U^* vs κa relationships for the heat treated latex shown in Table 1: in NaCl(●), $CaCl_2$(■) and $La(NO_3)_3$(▲) solutions at pH 5.5. The results for bitumen emulsions in NaCl(○) and $CaCl_2$(□) solutions at pH 5.5, carboxylated latex in $Ba(NO_3)_2$(■) at pH 7.7, and a silver iodide sol (●) in $1 \div 2 \times 10^{-2}$ M KNO_3 reported in refs.(this thesis chapter II), (4) and (33), respectively, are also included. The solid lines represent the theoretical U^*_{max} vs κa relationships for NaCl, $CaCl_2$ and $La(NO_3)_3$ solutions (15).

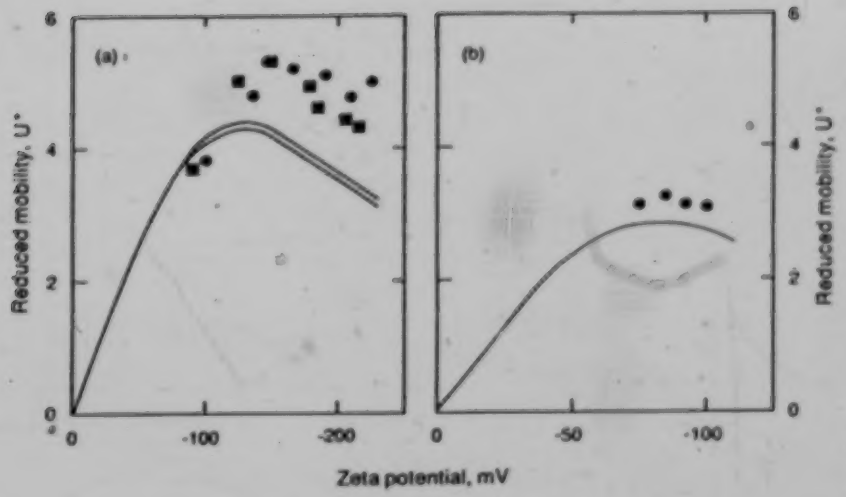

Figure III-5. (a) U^* vs ζ relationships for $26<\kappa a<30$ in NaCl solution, estimated from the measured U^* of a bitumen emulsion (■) and the heat treated latex (●) in 10^{-4} m NaCl. The solid lines represent the $U^*(\zeta, \kappa a)$ relationships calculated from O'Brien and White's computer solution (15).

(b) Same as (a) but for $\kappa a=36$ in 10^{-4} M NaCl solution in the presence of 3.0×10^{-5} M $CaCl_2$. The solid line is again from the computer solution.

REFERENCES

1. Takamura, K., and Chow, R.S., Colloids and Surfaces 15, 35 (1985).

2. Healy, T.W., and White, L.R., Adv. Colloid Interface Sci. 9, 303 (1978).

3. Harding, I.H., and Healy, T.W., J. Colloid Interface Sci. 107, 382 (1986).

4. Ottewill, R.J., and Shaw, J.N., J. Electroanal. Chem. 37, 133 (1972).

5. Wiese, G.R., James, R.O., and Healy, T.W., Disc. Faraday Soc. 52, 302 (1971).

6. Hunter, R.J., "Zeta Potential in Colloid Science," Academic Press, New York, 1981.

7. Douglas, H.W., Trans. Faraday Soc. 46, 1082 (1950).

8. Jordan, D.O., and Taylor, A.J., Trans. Faraday Soc. 48, 346 (1952).

9. Taylor, A.J., and Wood, F., Trans. Faraday Soc. 53, 523 (1957).

10. Carroll, B.J., and Haydon, D.A., J. Chem. Soc. Faraday 1, 71, 361 (1975).

11. Stachurski, J., and Michalek, M., Colloids and Surfaces 15, 255 (1985).

12. Yoon, R.H., and Yordan, J.L., J. Colloid Interface Sci. 113, 430 (1986).

13. Wiersema, P.H., Loeb, A.L., and Overbeek, J.Th.G., J. Colloid Interface Sci. 22, 78 (1966).

14. Goff, J.R., and Luner, P., J. Colloid Interface Sci. 99, 468 (1984).

15. O'Brien, R.W., and White, L.R., J. Chem. Soc. Faraday Trans. 2, 74, 1607 (1978).

16. Kawaguchi, H., Hoshino, H., Amagasa, H., and Ohtsuka, Y., J. Colloid Interface Sci. 97, 465 (1984).

17. Ohshima, H., Healy, T.W., and White, L.R., J. Chem. Soc. Faraday Trans. 2, 79, 1613 (1983).

18. Flory, P.J., "Principles of Polymer Chemistry," Cornell University Press, New York, 1953.

19. Stigter, D., Adv. Colloid Interface Sci. **16**, 253 (1982).

20. Israelachvili, J.N., J. Colloid Interface Sci. **110**, 263 (1986).

21. Ohshima, H., Makino, K., and Kondo, T., J. Colloid Interface Sci. **113**, 369 (1986).

22. Yates, D.E., Levine, S., and Healy, T.W., J. Chem. Soc. Faraday Trans. 1, **70**, 1807 (1974).

23. Davis, J.A., James, R.O., and Leckie, J.O., J. Colloid Interface Sci. **63**, 480 (1978).

24. James, R.O., Davis, J.S., and Leckie, J.O., J. Colloid Interface Sci. **65**, 331 (1978).

25. Davis, J.A., and Leckie, J.O., J. Colloid Interface Sci. **67**, 90 (1978).

26. Sharma, M.M., and Yen, T.F., J. Colloid Interface Sci. **98**, 39 (1984).

27. James, R.O., and Parks, G.A., "Surface and Colloid Science," Vol. 12, E.Matijevic, ed., Plenum, New York, 1982, pp.119-216.

28. Overbeek, J.Th.G., Adv. Colloid Interface Sci. **3**, 97 (1950).

29. Dukhin, S.S., Derjaguin, B.V., "Surface and Colloid Science," Vol. 7, E. Matijevic, ed.), Wiley, New York, 1974, pp.52-72.

30. Fixman, M., J. Chem. Phys. **78**, 1483 (1983).

31. Fixman, M., and Jagannathan, S., J. Chem. Phys. **75**, 4048 (1981).

32. Fixman, M., and Jagannathan, S., Macromolecules **16**, 685 (1983).

33. Troelstra, S.A., Thesis, Utrcht, 1941, p.105, referred in (14).

34. DeLacey, E.H.B., and White, L.R., J. Chem. Soc. Faraday Trans. 2, **77**, 2007 (1981).

35. O'Brien, R.W., and Perrins, W.T., J. Colloid Interface Sci. **99**, 20 (1984).

36. O'Brien, R.W., J. Colloid Interface Sci. **81**, 234 (1981).

37. Ohshima, H., Healy, T.W., and White, L.R., J. Chem. Soc. Faraday Trans. 2, **80**, 1299 (1984).

38. Zukoski, C.F., and Saville, D.A., J. Colloid Interface Sci. **107**, 322 (1985).

CHAPTER IV

GENERAL CONCLUSIONS AND SUGGESTIONS FOR FURTHER RESEARCH

1. General Conclusions

The general conclusions of this thesis are summarized below.

a. The technique of laser Doppler electrophoresis gives more accurate values of zeta potential. The prime reason for this is that the mobility measured can be correlated to the mean particle size. If an experimenter is working with a polydisperse emulsion, it is perhaps the best instrument to use for the determination of zeta potential.

b. One limitation of laser Doppler electrophoresis using narrowly gapped electrodes is the pH drift on the electrode surface. Although the drift can be controlled by the use of buffer, the buffer components should be carefully screened to find if they interact with the interface studied or change the ion concentration in solution by ion pairing or complexation.

c. The ionizable surface-group model can be used to predict the electric properties of the bitumen/water and Moutray crude/water interfaces in the presence of calcium or magnesium ion if the interaction between the surface group and the bivalent ion is included. The interaction can be modelled using the formation constant for acetic acid and the calcium ion.

d. Surface roughness must be considered when interpreting zeta potentials. For a rough surface, the distance to the surface of shear will be larger than if the surface was smooth. This will result in a lower zeta potential.

e.The current theory of the electrophoretic relaxation effect

overestimates its magnitude at low κa and high zeta potential. Until this problem with the theory is resolved, it is probably wise to avoid electrophoretic mobility measurements at $\kappa a < 100$ and at high zeta potential, although in most situations it is difficult to know the zeta potential in advance. If it is necessary to conduct measurements at $\kappa a < 100$ it may be best to measure the mobility of the substance, and if the electrophoretic mobility is close to the maximum predicted by the theory for that κa, the experiment should be redesigned.

2. Suggestions for Further Research

It has been shown that the computer solution of O'Brien and White overestimates the relaxation effect. The limits that the theory can be applied to may be found by repeating the experiments using heat treated latex of different sizes. Using smaller particles will allow for the testing of the theory at $\kappa a < 8$ while maintaining sufficient ionic strength to accurately define κ.

As shown in chapter 2, the charge at the oil/water interface originated from the dissociation of carboxyl groups. The total number of sites on the surface, Ns, can be roughly related to the acid number of the crude. Experiments should be conducted using other crude oils to discover if there is some explicit relationship between the acid number and the total number of groups on the surface.

The interaction between the Ca^{++} and the surface carboxyl group could be modelled by using a formation constant for acetic acid and the Ca^{++} that was determined in bulk solution. It would be interesting if this could be applied to other bivalent ions.

APPENDIX I

THE LASER DOPPLER APPARATUS

1. Advantages of Laser Doppler Electrophoresis

One of the advantages of using laser Doppler electrophoresis is that it is possible to correlate the mean size of an emulsion with a wide particle size distribution to the mobility measured by the laser Doppler apparatus. In principle if a large enough number of particles were measured, and the operator took care in selecting all the particle sizes this could also be accomplished using conventional microelectrophoresis. It would be a tedious endeavor, however.

Another advantage of laser Doppler electrophoresis is that the electrophoretic mobility of very small particles can be measured. For example Doppler spectra have been obtained for a gold sol that was ~ 25 nm in size. The resulting zeta potential was approximately 90 mV. It would not be possible to determine this by conventional electrophoresis because the particles are too small to see.

In principle, it is possible to obtain the mean particle size of a distribution of sizes. In the absence of an electric field, the half-width at half-height of the peak, Δf, centered at zero frequency is given by:

$$\Delta f = \frac{DK^2}{2\pi} \qquad [1]$$

$$D = \frac{kT}{6\pi\eta a} \qquad [2]$$

$$K = 4\pi(n/\lambda)\sin(\theta/2) \qquad [3]$$

where D is the diffusion constant which for a spherical particle of radius a in a medium of viscosity η is given by equation [2]. In equation [2] k is the Boltzmann constant and T is the absolute temperature. K is the scattering vector for radiation of wavelength λ in medium of refractive index n at angle θ. In the present configuration (scattering angle 16.2°) a particle of radius 0.8 μm would have a half width of 0.67 Hz. Unfortunately, the resolution of the spectrum analyzer is not sufficient to observe this. When the Brownian motion spectrum of the previously mentioned gold sol was measured, the half width observed did not correspond with the appropriate size. It was thought that some external vibration was interferring with the measurement. Further experiments are will be conducted to solve this problem.

2. Electrode Construction

The material selected for the electrodes was platinum, because it is inert and its surface area can be increased substantially by platinizing. This is important to avoid the generation of gas bubbles due to the electrolysis of water. Electrodes were obtained in dimensions of 2x2x15 mm. These were held in an acrylic holder.

Platinization was done with a commercially available platinizing kit (YSI #3139, YSI Inc., Colorado Springs, CO) generally a current density of 60 $mAcm^{-2}$ was applied for 3 or 4 minutes, switching the polarity every 30 seconds. This was followed by a thorough rinsing with distilled water.

The interelectrode distance must be accurately known as it is this parameter that determined the strength of the electric field. The distance was measured using a measuring microscope to ±0.01 mm.

3. Optical System

The design in use is very similar to the instrument used by Uzgiris. The TSI optics, however, offer significant advantages in comparison to the construction of the system with separate components. The largest advantage of the TSI optics is the ease of alignment. All the components are fitted into optical mounts that lock together in good alignment easily and quickly. In addition, mounts are available for most commercially available lasers that will raise the beam to a height that will be uniform for all the components. This eliminates the need to align the system vertically.

Another feature is that the beamsplitter in use splits the intensity of the incoming beam such that 0.5 % of the intensity is contained in one beam and 99.5 % in the other. This is done to achieve good ratios of scattered to reference light. In a system where the intensity is not split in such a manner, it is necessary to attenuate the reference beam using a neutral density filter.

The largest disadvantage of the TSI optics is the lack of an appropriate optical system that will result in scattering angles (in water) greater than 16°. There are, however, an excellent selection of lens that produce angles less than this. Unless very large particles are used, however, it should be possible to achieve a satisfactory angle.